LAPPEENRANTA UNIVERSITY OF TECHNOLOGY
Faculty of Technology
Energy Technology Degree Programme

Thermal Stress in a Roll-to-Roll Printed Electronics Substrate

The subject of this thesis has been approved by the Department of Energy Technology in Lappeenranta on the 29th of August 2012

Examiners: Professor, Ph.D. Esa K. Vakkilainen
Docent, Ph.D. Juha Kaikko
Supervisor: Research Engineer, M.Sc. Sauli Kivikunnas

Lappeenranta 6.11.2012
Hiski Hämäläinen

ABSTRACT

LAPPEENRANTA UNIVERSITY OF TECHNOLOGY
Faculty of Technology
Energy Technology Degree Programme
Hämäläinen, Hiski Eino Aapeli

Master's Thesis
2012
95 pages, 52 figures, 3 tables and 1 appendix

Examiners: Professor, Ph.D. Esa K. Vakkilainen
Docent, Ph.D. Juha Kaikko
Supervisor: Research Engineer, M.Sc. Sauli Kivikunnas

Hakusanat: Painettava elektroniikka, rullalta rullalle -painatus, terminen jännitys
Keywords: Printed electronics, Roll-to-Roll printing, thermal stress

Thermal Stress in Roll-to-Roll Printed Electronics Substrate

The Roll-to-Roll process makes it possible to print electronic products continuously onto a uniform substrate. Printing components on flexible surfaces can bring down the costs of simple electronic devices such as RFID tags, antennas and transistors. The possibility of quickly printing flexible electronic components opens up a wide array of novel products previously too expensive to produce on a large scale.

Several different printing methods can be used in Roll-to-Roll printing, such as gravure, spray, offset, flexographic and others. Most of the methods can also be mixed in one production line. Most of them still require years of research to reach a significant commercial level. The research for this thesis was carried out at the Konkuk University Flexible Display Research Center (KU-FDRC) in Seoul, Korea.

A system using Roll-to-Roll printing requires that the motion of the web can be controlled in every direction in order to align different layers of ink properly. Between printers the ink is dried with hot air. The effects of thermal expansion on the tension of the web are studied in this work, and a mathematical model was constructed on Matlab and Simulink. Simulations and experiments lead to the conclusion that the thermal expansion of the web has a great influence on the tension of the web. Also, experimental evidence was gained that the particular printing machine used for these experiments at KU-FDRC may have a problem in controlling the speeds of the cylinders which pull the web.

TIIVISTELMÄ

LAPPEENRANNAN TEKNILLINEN YLIOPISTO
Teknillinen Tiedekunta
Energiatekniikan koulutusohjelma
Hämäläinen, Hiski Eino Aapeli

Diplomityö
2008
95 sivua, 52 kuvaa, 3 taulukkoa ja 1 liite

Tarkastajat: Professori TkT Esa Vakkilainen
Dosentti TkT Juha Kaikko
Ohjaaja: Tutkimusinsinööri DI Sauli Kivikunnas

Hakusanat: Painettava elektroniikka, rullata rullalle -painatus, terminen jännitys
Keywords: Printed electronics, Roll-to-Roll printing, thermal stress

Substraatin lämpötilakäyttäytyminen elektroniikan rullalta rullalle –painatuksessa

Rullalta rullalle -painatus mahdollistaa jatkuvan elektronisten komponenttien tuotannon yhtenäiselle pinnalle. Komponenttien tulostus taipuvalle pinnalle voi halventaa RFID-sirujen, antennien ja transistoreiden tuotantokustannuksia. Joustavan elektroniikan nopea tulostus mahdollistaa useiden uusien tuotteiden valmistuksen joiden tuotanto oli ennen liian kallista isossa mittakaavassa.

Tulostettaessa rullalta rullalle voidaan käyttää useita erilaisia tulostus ja pinnoitus metodeja kuten gravuuri, suihku, offset, flexografia yms. Useimmiten metodeja voidaan myös sekoittaa samalla tuotantolinjalla. Useimmat näistä metodeista vaativat kuitenkin vielä vuosia tutkimusta ennen kuin kaupallinen tuotannon taso voidaan saavuttaa. Tutkimus tätä työtä varten tehtiin Seoulissa, Korean tasavallassa, Konkuk University Flexible Display Research Centerissä (KU-FDRC).

Laitteisto joka käyttää rullasta rullaan -painatusta vaatii yhtenäisen tulostuspinnan liikkeen tarkkaa jokasuuntaista ohjausta, jotta eri tulostuskerrokset sijoittuvat oikeille paikoilleen. Eri tulostusvaiheiden välillä muste kuivataan kuumalla ilmalla. Tässä työssä tutkittiin lämpölaajenemisen vaikutusta tulostuspinnan jännitykseen, ja tätä varten muodostettiin matemaattinen malli Matlabin Simulink-laajennuksella. Simulaatiot ja laboratorio testitulokset osoittivat että lämpölaajenemisella on suuri vaikutus tulostuspinnan jännitykseen. Koetulosten perusteella vaikuttaa myös olevan mahdollista että käytetyllä KU-FDRC:n koelaitteistolla on vaikeuksia pitää tulostuspintaa vetävien sylintereiden nopeuksia täysin tasaisina.

FOREWORD

I would like to thank Konkuk University, VTT Finland and VTT International Ltd., Korea Branch for the opportunity to travel to Korea and be a part of the research into technology that will be a big part of our everyday lives in the future.

I would also like to thank the thesis inspector, Sauli Kivikunnas from VTT, and my professor, Esa Vakkilainen, for giving me crucial advice on writing my work.

Also thank you to my family and friends for helping me to reach the end of my Master's studies!

Thank you and 감사 합니다!

Table of Contents

LIST OF SYMBOLS AND ABBREVIATIONS

Roman alphabet

t	=	Tension
A	=	Cross sectional area
E	=	Young's modulus
L	=	Length
x	=	Position in the length of the substrate
V	=	Velocity

Greek alphabet

μ	=	10^{-6} or micro
n	=	10^{-9} or nano
ρ	=	Density
ε	=	Strain
γ	=	Emissivity
σ	=	Stefan Boltzmann's constant

Superscript

e	=	Caused by elasticity
t	=	Caused by temperature
g	=	Glass (temperature)
m	=	Melt (temperature

Subscript

c	=	Cold i.e. the part with the lower temperature
e	=	Caused by elasticity
h	=	Hot i.e. the part with the higher temperature
i	=	Section of the dryer span
T	=	Caused by temperature
t	=	Caused by temperature
u	=	Infinitesimal element
x	=	Machine Direction position

Abbreviations

Ag	=	Silver
APET	=	Amorphous Poly(ethylene terephthalate)
cP	=	centipoise (0.1 Pa*s) or dynamic viscosity
CD	=	Cross Direction
dpi	=	Dots Per Inch
DC	=	Direct Current
DAQ	=	Data Acquisition
EPC	=	Edge Positioning Control
kgf	=	kilogram force = 9.80665 m/s2
KOPTRI	=	Korean Polymer Testing & Research Institute
KU-FDRC	=	Konkuk University Flexible Display Research Center
LCD	=	Liquid Crystal Display
MD	=	Machine Direction
m/min	=	metres per minute
mm / m	=	millimetres per metre
ms	=	1×10^{-3} seconds = milliseconds
PET	=	Poly(ethylene terephthalate)
PID	=	Proportional Integral Derivative

1 INTRODUCTION

Printed electronics is a constantly evolving field of technology. Electronics production is coming to an age where the limits of our physical world are coming closer. A transistor's component may be only 200 atoms wide (Pinto et al. 2012, 4-8). Meanwhile the number of transistors produced per integrated circuit is always rising by "Moore's law", doubling every two years (Moore 1965, 3). These two phenomena do not fit together, as there will be a limit to how small a silicon transistor can be. In order to make a processor any faster 10 years from now, silicon will have to be abandoned in favour of other types of processors such as quantum computers (Peckham 2012). On the other hand, one might ask why do we need faster computers and are faster computers really a necessary advancement for people in the future? Should electronics only be inside computers, phones and clocks, or could there be a world with electronics everywhere?

By printing transistors on various substrates such as glass, paper, plastic and fabrics, we can put transistors and electronic appliances into places where they could not exist in the past. Clothes can be produced with built-in batteries and invisible solar panels. A newspaper can be made on a rollable sheet of plastic (Figure 1); wallpapers or clothes could emit light; information about products can be printed on cardboard packaging, and huge commercial video screens could be made for a fraction of the price of a LCD screen. (Krumm & Clemens 2011, 333-341)

Figure 1. In the Sci-Fi movie 'Minority Report' newspapers are electronic and animated. (Spielberg 2002)

Moreover, printed electronics should not be considered a replacement for ordinary electronic manufacturing. Printed electronics offers new areas of interest for electronics manufacturers, where ordinary electronics was not feasible or even possible before. Printed sensors could revolutionize medical technology, just as computers changed libraries. Printed RFID tags (Figure 2) for price information could change the face of shops and markets for good. (Bock et al. 2007, 1540) Also, the development of new products can be much faster, since the development of the circuits and the components can be carried out in the same facilities, while today electronic parts are manufactured separately. (NANO 2010)

Figure 2. A printed antenna manufactured by the KU-VTT Joint Research Center in Seoul Korea.

It should be noted that printed transistors are a very new development. There are hundreds of organizations developing the technology. The first commercial products were sold as recently as 2009, but forecasts say that by 2020 the industry will grow from a 10 million to an 8 billion market. (NANO 2010)

1.1 Roll-to-Roll Printing

Roll-to-roll printing is a method of producing electronics. Roll-to-roll technology comes from paper printing and especially newspaper printing, where it is also commonly used. It is a method of moving the substrate from printer to printer in one continuous substrate. In electronic printing the substrate moves from roll-to-roll and in-between there are printers that make multi-layered prints. Multi-layering is necessary in order to build electronics like transistors and diodes. The printing inside the printer can be done in various methods such as gravure, offset and ink-jet printing. (Cheng & Wagner 2009, 20)

Roll-to-roll printing has its problems. While the substrate moves, it can stretch and move sideways on the rolls. This can influence the functionality and quality of the

multi-layered print, as the different layers may not be correctly positioned. Therefore researchers are trying to find out how to register exactly where the substrate is moving and to control its path so that the different layers are printed directly on top of each other. (Choi et al. 2010, 867) In this thesis, the heat expansion of the substrate is considered in relation to the tension and stress in the so called ‘web’, that is the roll-to-roll printing surface. A mathematical model was formulated and simulated on the computer. Verification of the model was carried out through experiments conducted at the laboratory of Konkuk University Flexible Display Research Center (KU-FDRC) in Seoul, Republic of Korea.

1.2 Thesis Parameters

In this thesis all the common elements of a roll-to-roll printed electronics system are discussed. The purpose of the work is to make a mathematical model for a roll-to-roll substrate’s tension concerning the tension from the roll’s motors that pull the substrate, and the heat that is emitted from the heater in the finalizing stage. The model will be created in order to assess the significance of the thermal expansion and change in elasticity on the tension of the web in the system. These results can be used in future research in order to produce a more accurate register control system for the printer.

The discussion of the electronic components, batteries and displays etc. that are to be printed on these substrates is omitted simply because they are not the subject of the research. Although there might be some variable effects of heat transfer from the different components assembled onto the substrate, these will not be discussed here and should be the focus of other more specific case studies. Likewise, although coating methods are important, only printing methods will be discussed here. Moreover, the discussion on different substrate materials is confined only to PET (Poly(ethylene theraphthalate)).

1.3 Thesis Structure

This thesis consists of a theory section and a section describing simulations and experiments. The theory section consists of basic descriptions of methods, materials and technologies to print electronics. In the section describing experimental work, the mathematical modelling, simulation and the running of the tests as well as the printer conditions and experimentation devices are discussed in depth. At the end of the thesis the results, conclusions and suggestions for future research topics are presented.

2 METHODS AND MATERIALS OF PRINTED ELECTRONICS IN ROLL-TO-ROLL PRINTING

Printed electronics work in the same fashion as regular electronics, but are manufactured in a different fashion.

2.1 A Brief History of Printed Electronics

The first transistor was invented in 1947. The first transistors (Figure 3) were so big you could fit maybe one or two in your hand, while today the measurements of the different parts of the transistors are calculated in hundreds of atoms. Nowadays there are around 10 000 transistors produced per day per person on earth, therefore the research into making more transistors at one time more cheaply has become important. Due to constant developments, the costs of a function have gone down by 30% per year. (Pinto et al. 2012, 4-8)

Figure 3. The first transistor built. It was so big you could hold it in your hand. (Pinto et al. 2012, 2)

Today printed electronics is a subject of great interest to companies and researchers because it opens up possibilities never seen before. Printed electronics can reduce the

costs drastically and speed up the production of electronics immensely. (Krumm & Clemens 2011, 334) In the 1960s the first flexible photovoltaic solar cells were developed to be put onto a space ship, where it was important for the solar cell to be efficient and lightweight. The silicon solar cells were so thin that they bent from a change in temperature. This was the first flexible electronics made. In the 1970s the energy crisis fuelled research into thin-film solar cells in order to reduce the cost of solar energy. By the 1980s the roll-to-roll production of solar cells had started and today it is common practice. (Cheng & Wagner 2009, 1-2)

2.2 Methods of printed electronics

There are many different printing methods for printed electronics, such as screen printing, inkjet printing and gravure printing. Some of them can be done sheet by sheet, and some of them have to be done roll-to-roll. The sheet by sheet method means that each batch has to be prepared for the printer separately. In laymen's terms, roll-to-roll printing simply means that a long printing substrate is in a reel (Figure 4) that delivers the substrate into a printer and back onto another reel.

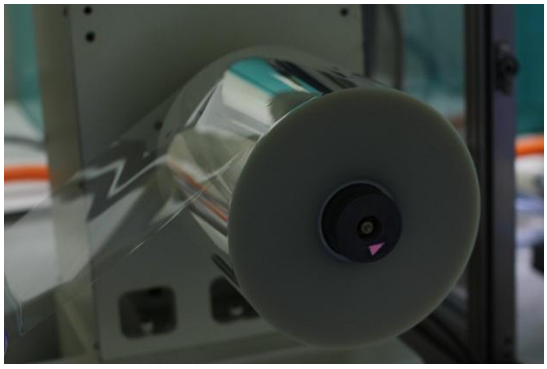

Figure 4. Infeeder cylinder of a roll-to-roll printing machine.

The main idea is still that there is a substrate onto which the components are printed, and that after printing there is usually a process whereby the components are either laminated or sintered, which both usually require heating. The temperature of this finalizing stage depends on the substrate's properties (Table 1) as well as the ink that is being used. The ink requires a certain temperature and the substrate is able to handle only a certain temperature.

Table 1. Printing method speed comparisons.

Printing technique	Print resolution [µm]	Print speed [m min^{-1}]	Wet film thickness [µm]	Ink viscosity [mPa s]
Flexo	30–75	50–500	0.5–8	50–500
Gravure	20–75	20–1000	0.1–5	50–200[a)]
Offset	20–50	15–1000	0.5–2	20 000–100 000
Screen	50–100	10–100	3–100	500–50 000[b)]
Inkjet	20–50[c)]	1–100[d)]	0.3–20	1–40[d)]

There are two different main categories of electronics printing. In coating, the idea is that it does not form a pattern but a smooth surface i.e. a layer. In printing, a definite pattern is formed on the substrate. (Krebs 2009, 398) On the other hand, when necessary, coating and printing can also be mixed. In these studies we will only delve into printing methods.

2.3 Contact Printing Methods

Contact printing comprises methods where the structure that is deploying the ink touches or is in pressure contact with the substrate.

2.3.1 Gravure Printing

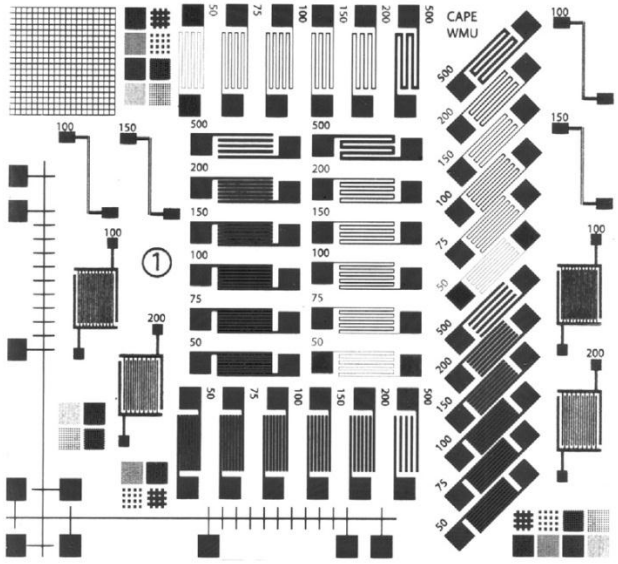

Figure 5. Example of a gravure printing model used to test silver inks. (Hrehorova et al. 2011)

In the gravure printing mechanism (Figure 6), there are two rolls, one of which is dipped into the ink, and the other is called the impression cylinder. There is also a "doctor blade" that removes the excess ink before the part that is inked reaches the substrate. The impression cylinder can for example produce such patterns as the one seen in Figure 5. When the system holds several of these printing cycles, it is possible to form different parts such as transistors and diodes by stacking up electrodes, semiconductors and insulators on top of each other in patterns (Krumm & Clemens 2011, 335)

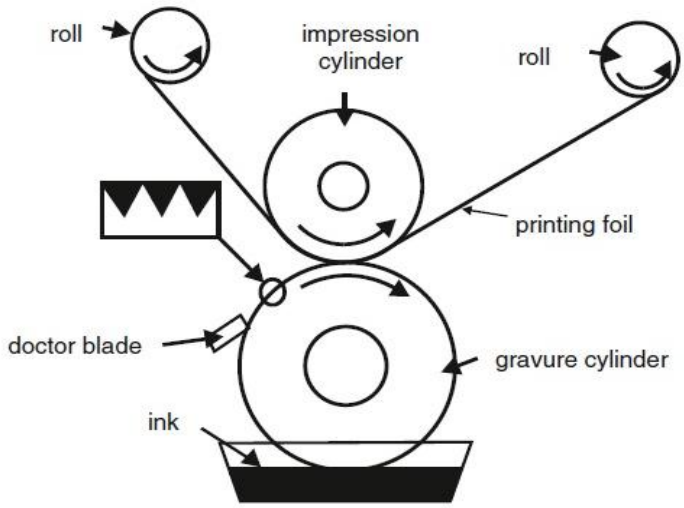

Figure 6. Operating principle of gravure printing. (Krumm & Clemens 2011, 334)

2.3.2 **Offset Printing**

Offset printing is widely used in printing newspapers. It works by having a plate with a gravure (Figure 7), which is covered by ink. The extra ink is carved off with a doctor blade and a roller with a blanket is rolled over the gravure. Then the roller is rolled over the substrate, and the ink is then transferred to the substrate. (Pudas et al. 2002)

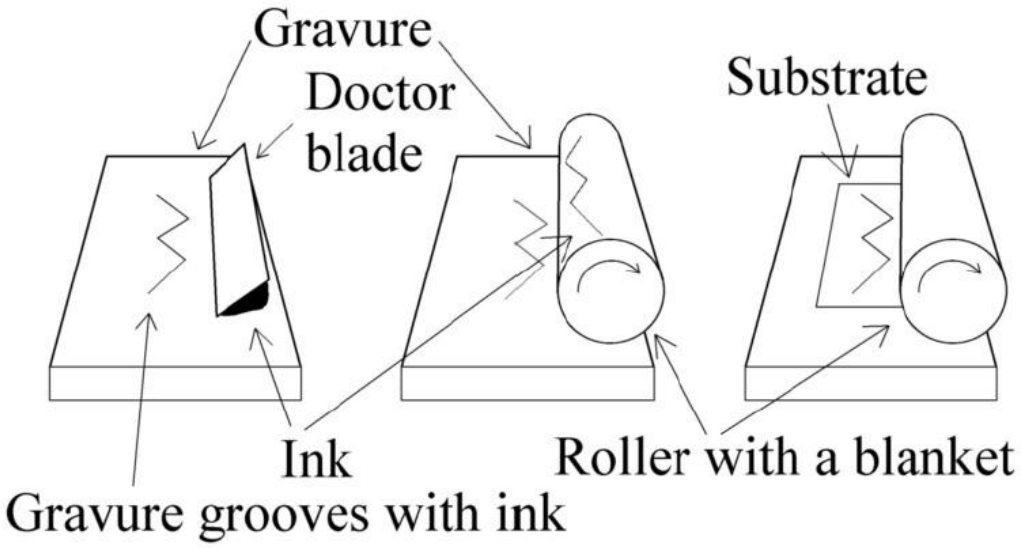

Figure 7. Offset printing basics (Pudas et al. 2002, 335)

2.3.3 **Photolithography and Nano Imprint Lithography**

In photolithography a copper laminate is coated, and exposing the coating to light through a desired screen results in a photo printed pattern which is then acquired into an electrically working pattern through a complicated process. (Numakura 2008, 205)

Nano imprint lithography is a similar process, but it can produce a nano-scale print. Here the mould is made of a transparent material. The ultraviolet light-sensitive ink is applied onto the substrate, and the mould is pressed against the substrate and the ink. Then the UV-light is applied, and the ink will cure and form the desired circuit. It is also possible to form circuits on the other side of the substrate. (NANO 2010)

2.3.4 **Screen Printing**

Screen printing is a process often used in making t-shirts and posters. It involves acquiring a screen with holes in the required pattern (Figure 8). The screen is held

against the substrate and the ink is pushed through the screen pattern. After that the pattern must be baked.

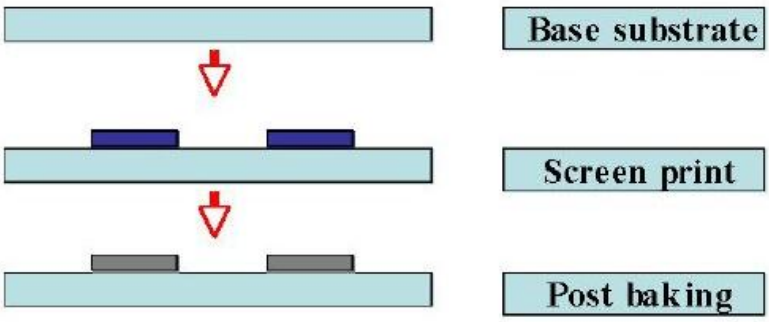

Figure 8. Screen printing process. (Numakura 2008, 205)

Screen printing is also used in printed electronics. According to Numakura (2008, 205), modern screen printing devices can print lines and spaces up to 10-20 µm in width or length. Screen printing can be used in a batch process sheet by sheet or with a rotary screen printer in a roll-to-roll process. (Tobjörk & Österbacka 2011, 1945) Screen printing can be used to print multiple layers as well as for double-sided printing and connections through the substrate by making holes in it. (Numakura 2008, 205)

In roll-to-roll screen printing, the screen is fixed onto the outside of a cylinder (Figure 9), and the ink is squeezed through the holes from the inside out, on to the substrate. (Krebs 2009, 401)

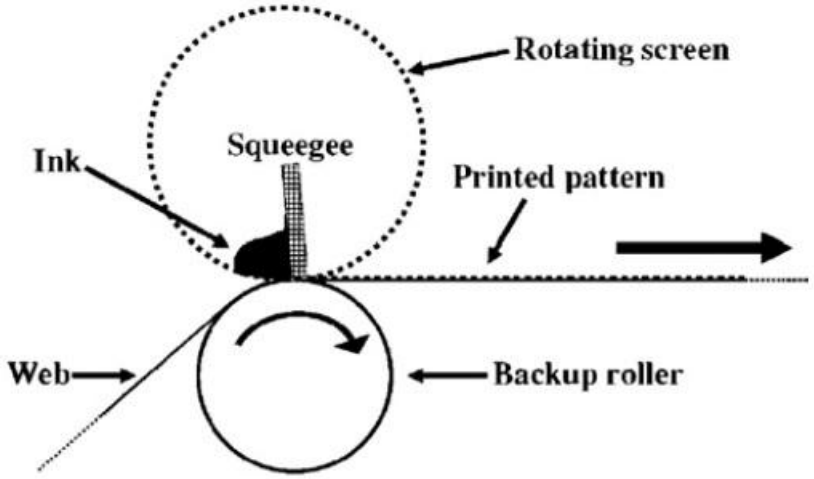

Figure 9. A rotating screen printer. (Krebs 2009, 401)

2.3.5 **Flexographic Printing**

Flexographic printing, often abbreviated to flexo, is a more advanced version of the rubber stamp or letterpress printing methods. With flexographic printing you can print on almost any kind of materials, including non-porous materials. The ink is transferred by the anilox to the plate roller (Figure 10), which carries it to the substrate. The anilox holds a specific amount of ink. The plate roller receives the ink on its protuberances and presses it onto the substrate with the help of the impression roller. (Keng et al. 2011, 517)

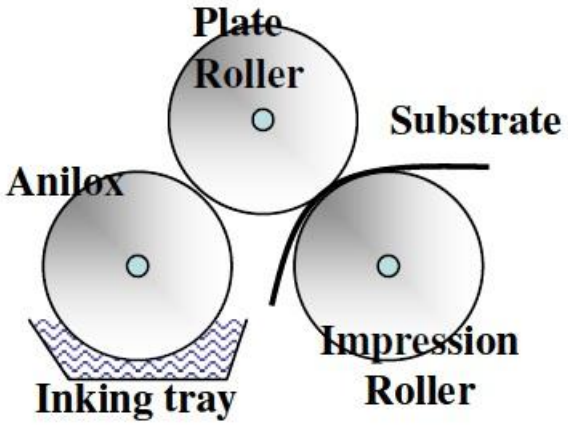

Figure 10. Flexographic printing. (Keng et al. 2011, 517)

Flexographic printing has a lower printing resolution than the very similar gravure printing, because as the flexible roll prints on the substrate there is a danger of distortion. (Tobjörk & Österbacka 2011, 1945)

2.3.6 **Offset Lithography**

Offset lithography is a method that is a standard in printing books. The name resembles photo-lithography but is actually quite different. Offset lithography is compatible with roll-to-roll printing; it is capable of very high speeds and line widths of less than 25 µm. (Southee et al. 2007, 4, 5)

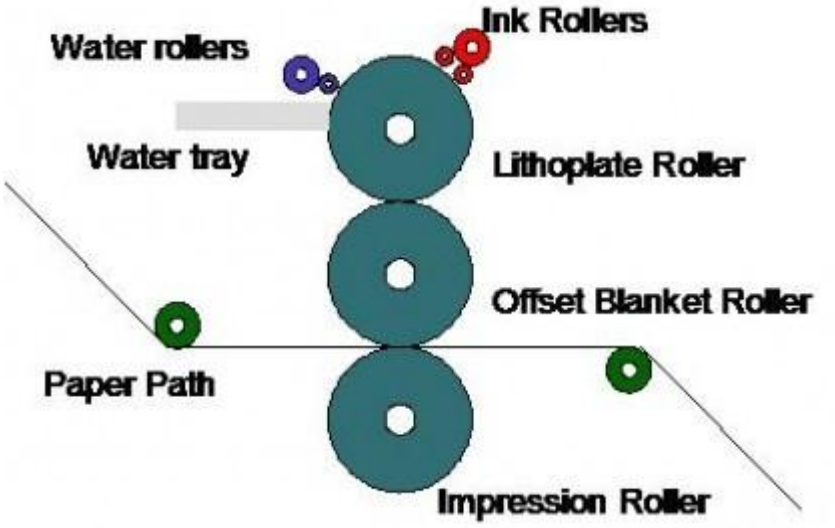

Figure 11. Offset lithography schematics. (IDTechEx 2012)

Lithography in Greek means "stone writing", which was an old method of printing, where the desired pattern is first drawn with an oil-based crayon onto a stone, which is then covered with water. The water will not attach to the oil-based markings, but will be on the stone. After that, ink is poured onto the stone, and while the water repels the ink, it will stay on the oil-based markings. After this a paper is put on top to make the print onto the paper. In offset lithography instead of the stones we have rollers. The first one receives the water and the ink. The second roller is an offset blanket roller (Figure 11) and it transfers the ink patterns onto the substrate. This way the pattern is mirrored twice, and it will look the same on the first roller and on the substrate. (IDTechEx 2012) In offset lithography, the viscosity of the ink can be quite high, from 30-100 Pas. (NANO 2010, 13)

2.4 Non-Contact Printing

In non-contact printing, the construction making the print does not touch the substrate.

2.4.1 Ink-Jet Printing

As mentioned earlier, the roll-to-roll gravure process can produce large volumes quickly, but because of the custom-made gravure cylinders it is quite rigid, and manufacturing new rolls for new applications is costly. A faster response to demand but a slower production can be met by ink-jet printing. A table-top machine (Figure 12) can print nanoparticles of aluminium and other metals with great precision. (Suganuma et al. 2007, 4) The print resolution can easily range from 300 dpi to 1200 dpi. Also, the advantage of the machine compared to most electronic printing methods is that it does not need a master image. The desired pattern can be designed on the computer which sends commands directly to the printer. (Krebs 2009, 401)

Ink-jet printing meets a lot of the demands of pattern printing of flexible electronics. It is compatible with roll-to-roll printing and with low-temperature processes and large area printing; it has easy registration and can even be adjusted in real time in order to realign to previous layers (Yin et al. 2010, 3385). Also, ink-jet printing is very compatible with organic materials (Yang et al. 2000, 95-96).

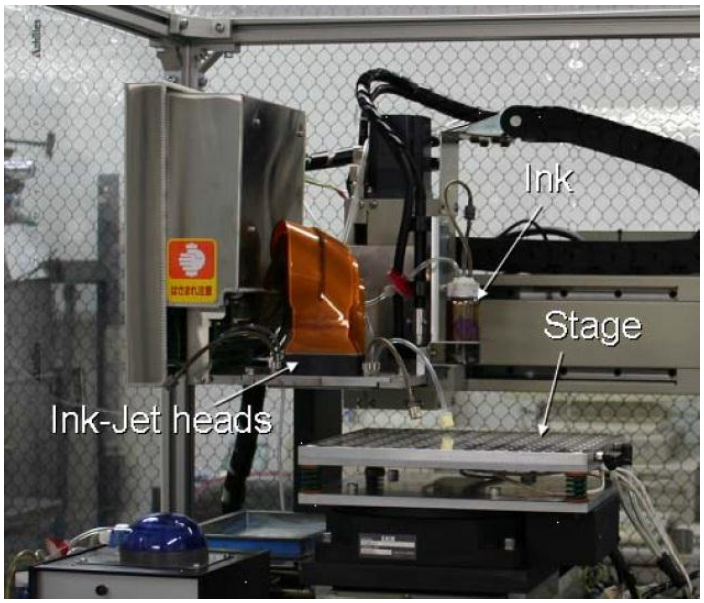

Figure 12. A tabletop inkjet printing machine. (Suganuma et al. 2007, 1)

As well as on-demand production, inkjet printing offers environmental awareness, because it does not produce as much waste as most other forms of printing. Also, it has the possibility to print in three dimensions and allows a wide selection of materials. (Suganuma et al. 2007, 1)

The ink is pushed out of the nozzle either by mechanical pressure or by heating the ink, which then expands and is extruded through the nozzle. After the nozzle there is an electric field which accelerates the electrostatically charged droplet towards the substrate. (Krebs 2009, 401)

In inkjet printing the viscosity of the ink must be kept low, or otherwise clogging may occur. This causes the ink to dry slowly, and finding the right ink viscosity and nozzle size (Figure 13) can take a lot of time. The smaller the nozzle, the more precise the printing gets, but the more difficult it is to maintain the system. (Tobjörk & Österbacka 2011, 1946)

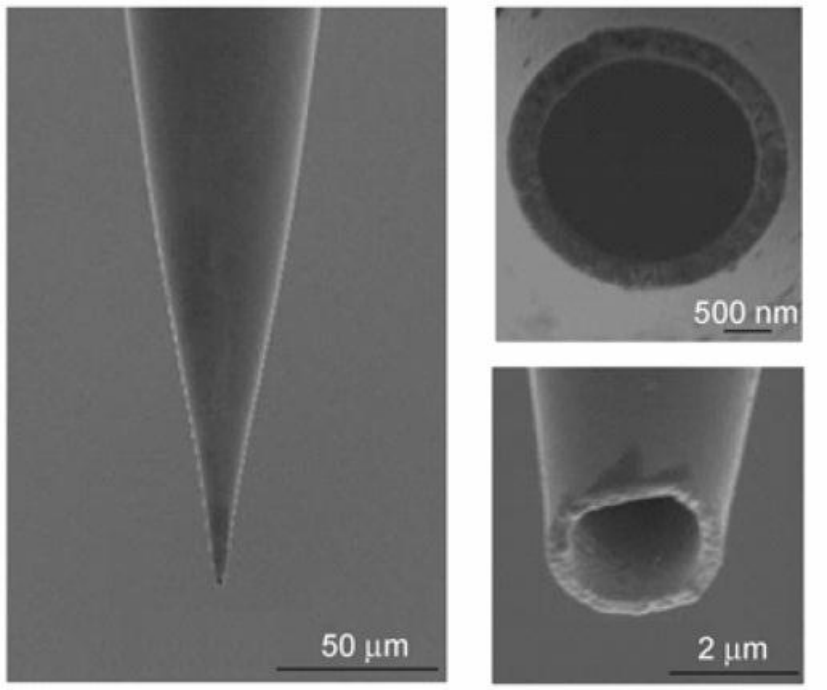

Figure 13. An ink-jet printing nozzle. (Yin et al. 2010, 3398)

2.4.2 **Spray Printing**

Spray printing is a technology that employs a carrier gas that pulls the ink under negative pressure up the pipe and through a nozzle onto the substrate. There can also be a separate sheath gas that prevents clogging in the nozzle. In Optomec's devices (Figure 14), the size of the smallest droplets are 10 µm, and the dynamic viscosity can be as high as 1,000 cP, while in an ink-jet printer the ink must be of low viscosity. (Optomec 2006a)

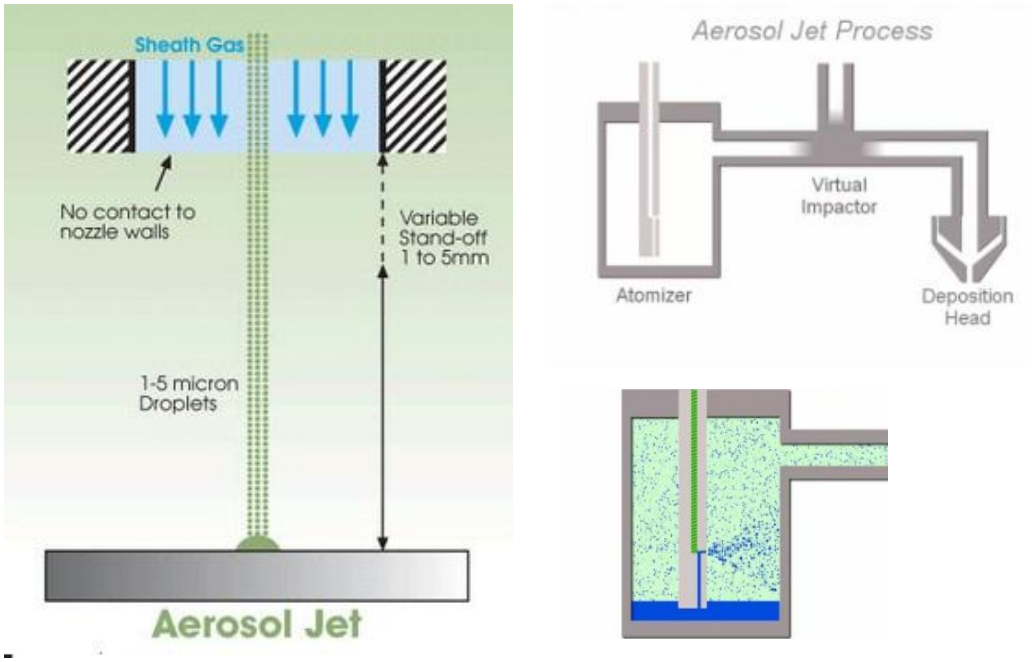

Figure 14. Sheath gas and droplet formation on the left (Optomec 2006a), aerosol jet process at the top right, and aerosol formation at the bottom right (green is the carrier gas, while blue is the ink). (Optomec 2006b)

2.5 Other Methods of Printed Electronics

There are other lesser known printing methods such as aerosol-jet printing, which has quite a high resolution of 10 µm and a speed of 12 m min^{-1}. A similar solution to inkjet printing is a liquid (micro) dispensing printer that is able to output a continuous stream of material through its nozzle instead of the inkjet printer's drop by drop method. Another method well known in paper printing is electronic laser printers. The lasers are only used to refine the printed electronics by heating up specific areas and then possibly washing away the remaining ink. This printing method is quite expensive. The Xerox principle can also be used in electronics printing. The problem with a Xerox machine lies in the fact that it produces lots of static electricity and heat. (Tobjörk & Österbacka 2011, 1946-1947)

2.6 Roll-to-Roll Printing

In roll-to-roll gravure printing the substrate is flexible and is rolled onto an infeed reel, from which it travels through the printing mechanism onto the rewind reel. The substrate in roll-to-roll systems is often called a web (Krebs 2009, 403). In the printing mechanism, the system consists of the infeeder to the printer, printer, dryers (by heat), a cooling mechanism and the outfeeder back onto a reel. Other processes involved may include cleaning of the web, removing static electricity, especially from plastic surfaces, and treating the web with UV-light (Krebs 2009, 403). Typically, the drying process has a temperature from 50 ºC to 300 ºC, depending on what kind of a temperature the ink requires in order to dry.

As the temperature of the substrate rises, its Young's modulus changes. Usually it gets smaller, which means the substrate becomes looser and more flexible. As the length and properties of the substrate change, the tension in the substrate changes, and it can cause wrinkles, creases (Figure 15), buckling and register errors. (Lee et al. 2009, 1907)

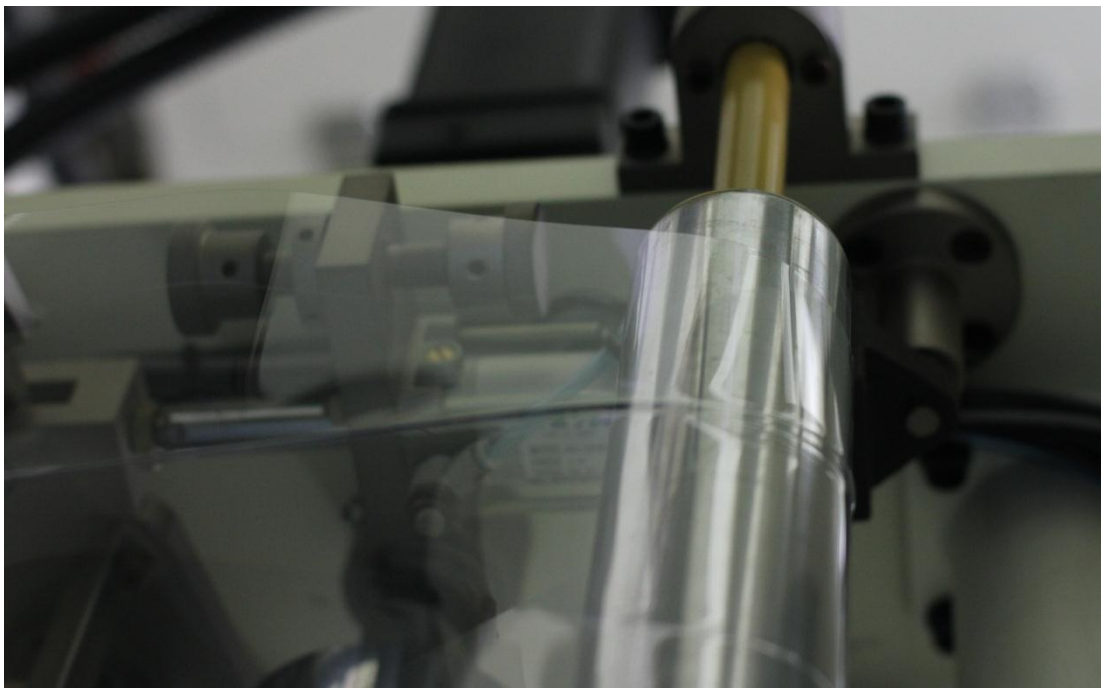

Figure 15. The web of the roll-to-roll machine at KU-VTT laboratories has a crease due to the lateral behaviour of the web.

It should be noted that roll-to-roll is a process to produce electronics (Figure 16) as well as any other kind of prints. It is not a printing method, as there can be several different methods like gravure or screen printing used within a roll-to-roll system. Nevertheless, there are printing methods that are not compatible with roll-to-roll.

Also, one should remember that the size of the heater is in relation to the speed of the system. So if a high speed system is required, a big and long heating unit is required as well for sintering. This can increase the costs a great deal. (Krebs 2009, 403)

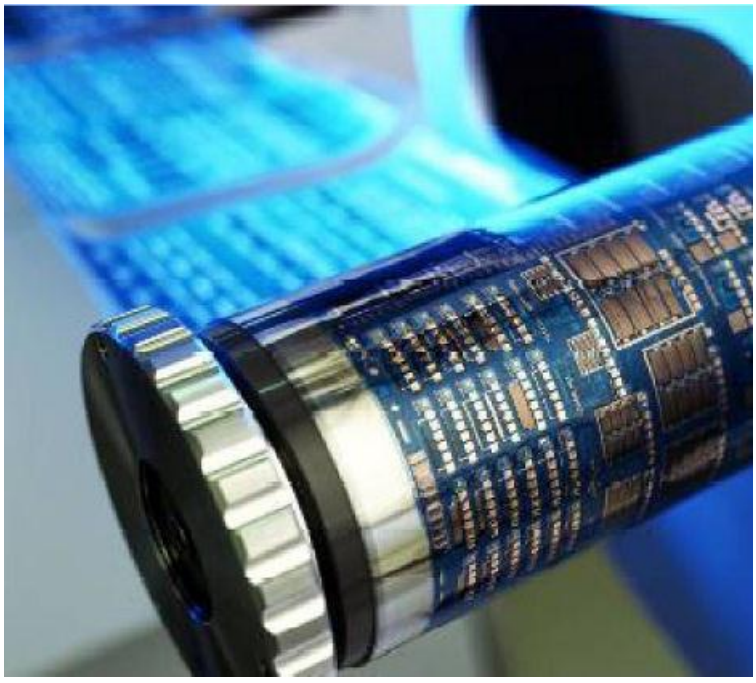

Figure 16. A completed roll-to-roll test chip at rewind stage in Germany. (Bock et al. 2007, 1543)

A roll-to-roll printer usually prints several layers of ink in order to produce functional electronics. This means that, while the substrate goes through one printing part to another, the printer has to know the exact position of the substrate in order to print the second layer directly on top of the previous one. A mistake in the layered printing position is called a register error (Figure 17). Register errors come in machine-

directional (MD) and cross-directional (CD) errors. Machine direction means the direction where the substrate is directly moving and cross-directional is when the substrate moves sideways. (Kang 2000, 391)

To control the tensions of the substrate one can control the speed of the rolls and the temperatures close to the printing substrate.

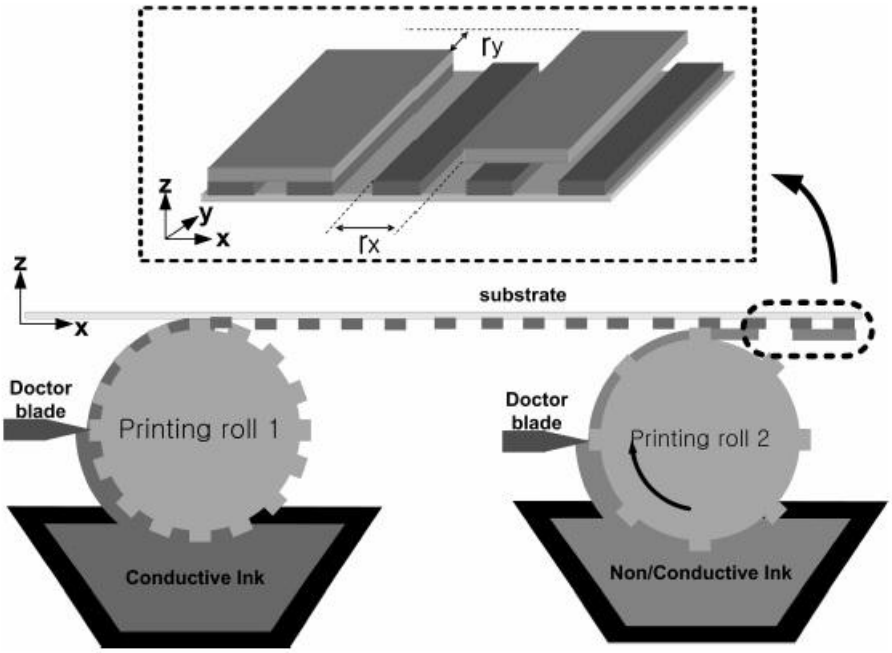

Figure 17. An illustration of the register errors r_x (MD) and r_y (CD). (Kang 2000, 2)

2.6.1 **Benefits of the Roll-to-Roll Process**

The roll-to-roll process is a method for cost-effectively producing electronics on a mass production line. (Kim et al. 2011, 690)

2.6.2 **Challenges of the Roll-to-Roll Process**

The roll-to-roll process is a good investment when the printing needs are for only one specific kind of product. A roll-to-roll system takes up a lot of space; it is very

expensive and it can usually use only one method of production, for example gravure. Nevertheless, a multi-purposed roll-to-roll printing system can be created in which gravure, gravure-offset and flexo printing methods can be used at the same time (Kim et al. 2011, 690). Roll-to-roll electronics printing is also still very much in a development phase, and different technologies are still being tested and researched.

2.6.3 **Materials Used in the Roll-to-Roll Process**

Materials used in roll-to-roll processes need to be flexible. Many materials have been used in printed electronics in the past, from thin silicone to thin glass, paper and different metals. In this thesis we will confine our studies only to PET type plastic.

2.7 PET or Poly(Ethylene Terephthalate)

PET polymers (Figure 18) were discovered by J.R. Whinfield and J.T. Dickson at DuPont in 1941. PET was found to be a good material for fibres. (Kutz 2011, 13). It is used in various everyday products such as beverage bottles because it has good strength properties. (Kutz 2011, 5). Concerning this thesis, PET is the material used in the experiments at KU-FDRC. The study of PET's structure is important for understanding the changes in elasticity and expansion at different temperatures.

Plastic (originally Greek "plastikos") is an adjective to describe materials that can be moulded. Often plastic is referred to as a polymer, but actually plastic materials are comprised of polymers and other additives like colours, i.e. plastic is a product of polymers and other substances. A polymer is a material composed of very long connected molecules that have the same main part repeating thousands of times to create long chains. (Kutz 2011, 3)

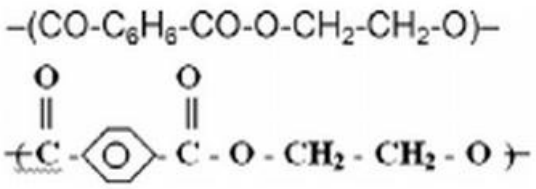

Figure 18. PET or poly(ethylene terephthalate) repeating chemical unit. (Kutz 2011, 5)

2.7.1 PET Elastic Properties

Considering the thermal properties of polymers, it should be noted that there are thermoplastic and thermoset polymers. As the names already indicate, the thermoplastic polymers, such as PET, can be moulded when heated, and so they are recyclable. The molecules in a thermoplastic polymer are separated, while in thermoset polymers the polymer chains are connected to each other. Thermoset polymers are stronger, but cannot be melted and changed back into another shape. Therefore, thermoplastic polymers are popular in consumer products such as bottles. (Kutz 2011, 3)

The thermal and strength properties of polymers are usually not linear as a function of temperature. A polymer can either be completely amorphous or semi-crystalline, but so far there are no completely crystalline polymers. When a polymer is semi-crystalline, a proportion of its molecules are aligned into layers, and the rest are not in any specific order or form. PET can be heat-processed into an amorphous PET (APET), but usually it is semi-crystalline. The crystallization of a polymer is induced by slowly lowering the temperature. (Kutz 2011, 3, 5).

So there are two important temperatures for a polymer, its glass and melting temperature. After reaching the glass temperature the amorphous parts become loose, and after reaching the melting temperature the crystalline parts also become loose. Figure 19 shows what happens to a semi-crystalline polymer when it is heated. (Kutz 2011, 3)

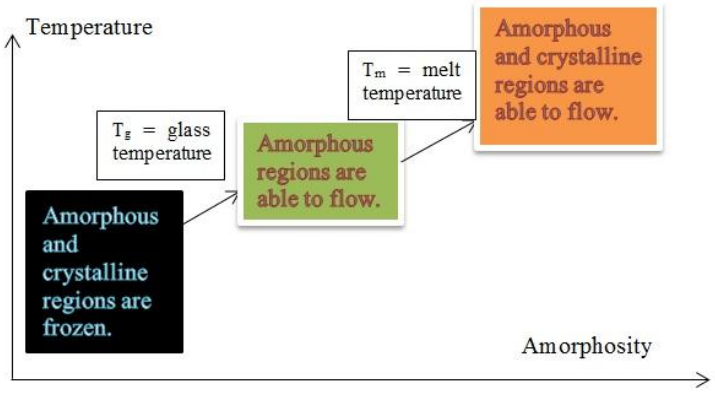

Figure 19. The above figure describes the different stages of behaviour of a semi-crystalline polymer at different temperatures.

It should also be noted that an amorphous polymer does not have a T_m melting temperature because it has no crystals. Generally PET's glass temperature point T_g = 70 ºC. (Kutz 2011, 3). For an amorphous PET, the T_g = 67 ºC, in a semi-crystalline state T_g = 81 ºC and in a crystalline state T_g = 125 ºC. PET's melting temperature T_m varies in the range of 250 – 265 ºC. (Sabu & Visakh 2011, 103)

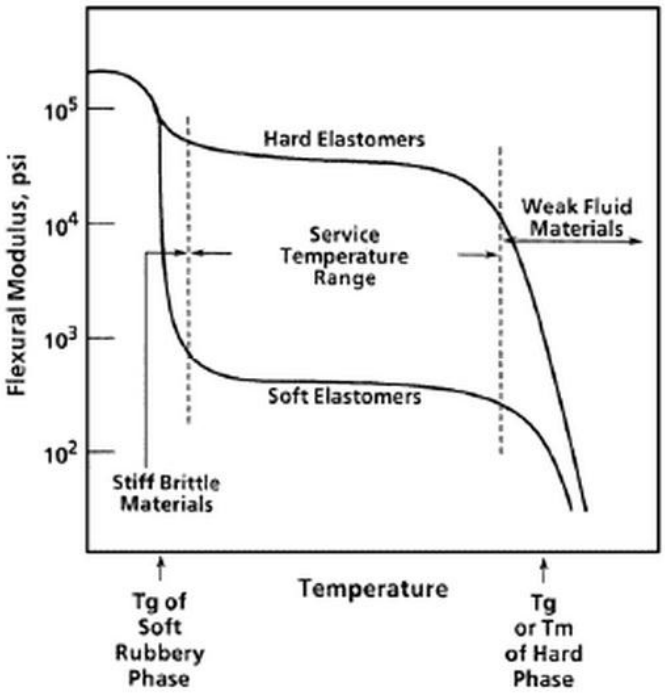

Figure 20. The elastic modulus in relation to the temperatures of a thermoplastic polymer. (Kutz 2011, 83)

The "flexural modulus" (Figure 20), better known as the elastic modulus (E), is the measure of stiffness in a material. The higher the number of the elastic modulus, the stiffer the material is. From the figure we can determine that the higher the temperature of a thermoplastic material, the less stiff the material gets. At lower temperatures the material is stiff, but when heated it becomes elastic. When it reaches the melting temperature T_m, the polymer's stiffness declines rapidly, and if pulled the material would probably collapse.

2.7.2 **PET Thermal Expansion**

It is difficult to find information on PET's thermal expansion properties in literature. This is because the coefficient is non-linear, and at one point it even changes from expansion to shrinkage. The polymers are a complicated matter, and when the structure

starts to break under heat, the PET polymer starts to shrink. More information will be given on this in the model building and verification part of this work (Ch. 3).

2.7.3 PET or Poly(Ethylene Terephthalate) Mechanical Properties

As mentioned before (Ch. 2.8) the amorphousness of PET depends on how it is fabricated. The amount of crystallisation then affects the strength properties of PET (Figure 21). When PET cools down it starts to crystallize, but the process is slow. Therefore, if rapidly cooled, PET will stay amorphous even at a cooler temperature. (Sabu & Visakh 2011, 102, 103)

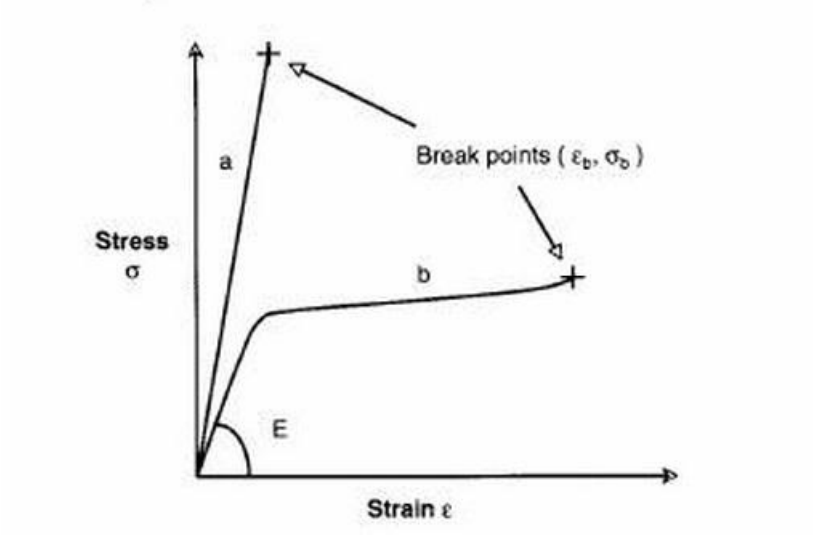

Figure 21. Stress-strain relation of (a) brittle polymers and (b) soft polymers. (Sabu & Visakh 2011, 102)

Strain represents the length the polymer has been stretched (ΔL) in relation to its full length (L).

$$\varepsilon = \frac{\Delta L}{L} \quad (1)$$

Stress is the tensile stress, pressure or pulling force divided by cross section area that affects the polymer.

$$\sigma = \frac{F}{A} \qquad [N/m^2] \text{ or } [Pa] \qquad (2)$$

Here we can also observe Hooke's law, which explains the connection between the elastic modulus E, and strain or force.

$$\sigma = E\varepsilon \qquad [N/m^2] \text{ or } [Pa] \qquad (3)$$

When multiplied by the cross-sectional area A, becomes (Sadd 2009, 519):

$$F = EA\varepsilon \qquad [N] \qquad (4)$$

A soft polymer will stretch much more than a brittle one. Brittle polymers take a lot of stress, but will not stretch as much. Whether a polymer is brittle or soft results from complex reasons including heating, amorphousness and added fibres. Table 2 represents a few values of PET films at different statuses from a handbook on thermoplastics. (Sabu & Visakh 2011, 103)

Table 2. PET mechanical properties in different states. (Sabu & Visakh 2011, 103)

PET sample	Amorphous		Semi-crystalline	
	Non-loaded	Loaded with 20 % glass fibers	Non-loaded	Loaded with 20 % glass fibers
Modulus of elasticity, E (GPa)	2	5	2.4	5.6
Ultimate tensile strength, s_r (MPa)	45	114	38.5	138
Elongation at break, ε_r (%)	250	3	90	3

From the table we can see that the elastic modulus and, therefore, the stiffness of the polymer can even be doubled by adding glass fibres to it. What is more, we can see that a semi-crystalline polymer is stiffer in its elasticity, but at the same time its ultimate tensile strength is lower and its breaking point of strain is much lower than the amorphous PET, which is as predicted by the Figure 21 explaining the stress-strain relations of PET. This means that the semi-crystalline polymer is a brittle polymer and the amorphous one is soft.

2.8 Flexibility in Printed Electronics Products

Printed electronics offers a chance to make electronics cheaply, but another exciting feature is the possibility of producing flexible electronics. The roll-to-roll process naturally requires the substrate to be flexible, but there are different degrees and styles of flexibility. Flexibility can mean that:

1) The product will not break when bent or rolled up (like a newspaper).
2) The product can plastically deform, i.e. remain functioning after a permanent change of shape or length.
3) The product can stretch, i.e. it is elastic and is able to return to its original form after deformation. (Cheng & Wagner 2009, 3,4)

Different types of flexibilities offer many possibilities as regards products. A roll-able electronic newspaper (Figure 22) could save people from wasting printing paper. In 2008 the newspaper industries alone cut down 125 million trees world-wide, and are responsible for huge amounts of waste water from the processing of the paper (Singh 2010). This is a good example of a future technology that solves the problems of past ones.

Figure 22. An electronic newspaper could save over a hundred million trees per year. (Singh 2010)

Plastically deformable electronics could remain functional after an accident, for example in a phone or a car. Stretchable electronics could offer endless possibilities for the clothing industry from displays on clothing to having solar panels and batteries inside or on top of the fabric of the clothes. For example, a police vest was developed in Thailand by Tunlasakun and Makasorn (2008, 1337) which featured a flexible solar panel as well as a flexible lamp (Figure 23), making the policeman's clothing a functional self-sufficient piece of safety kit.

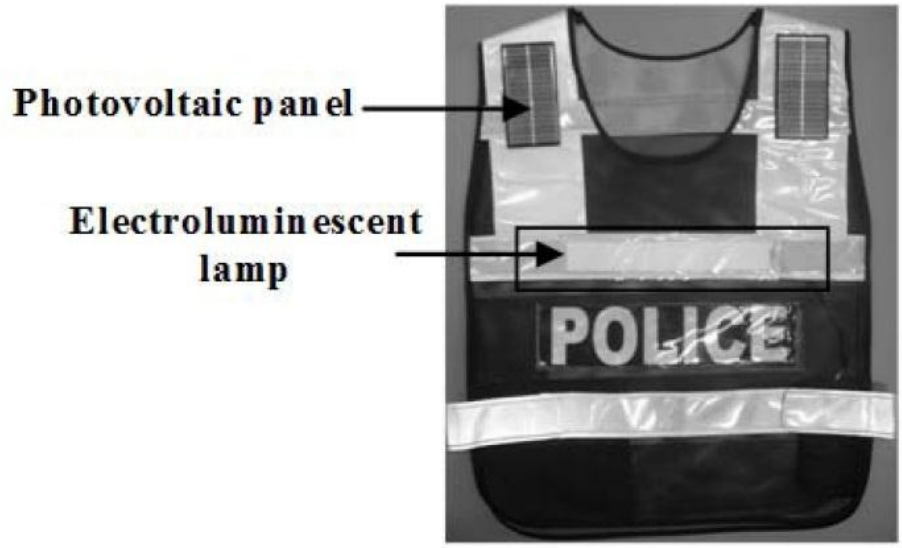

Figure 23. A self-powering illuminated police vest. (Tunlasakun & Makasorn 2008, 1338)

In stretchable fabric prototypes of Löher et al. (2008, 12), the stretchability was produced by shaping copper connectors into horseshoe shapes through the fabric. They were able to stretch the fabric without breaking even up to 300% at a time.

Mobile phones are one of the most interesting solutions for implementing flexible electronics. It is a well-known fact that the screens of modern phones break easily, but if the screen and the electronics inside were flexible, the device would be practically indestructible. A prototype of a flexible mobile phone was shown by Nokia in October 2011 (Figure 24). According to the website GSM-Arena, it also featured a user interface where in order to zoom the picture or scroll down, the user could actually bend the phone in different ways. (Arena 2011)

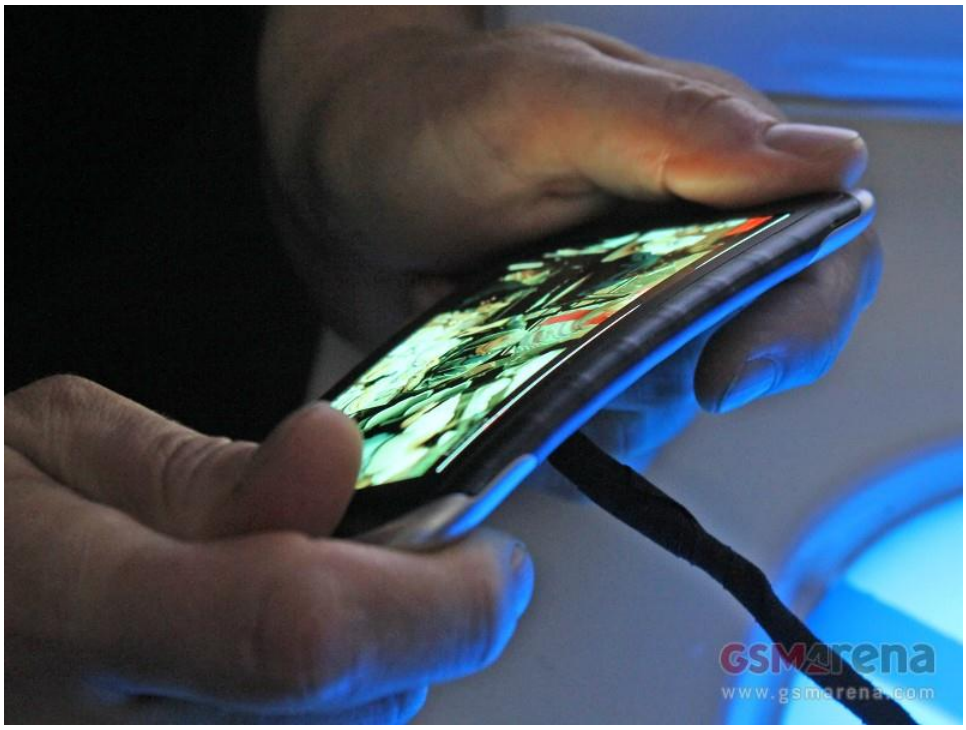

Figure 24. A Nokia prototype mobile phone that uses its bendability to operate the phone. (Arena 2011)

The problem with mobile phones today according to McGoldrick (2006, 1) is that they are changing from being merely phones into data devices. This abundant data needs to be shown on a bigger screen, but a bigger screen requires a bigger device. At that time it was suggested that a rollable screen could make for a small device with a big screen. In 2007 the iPhone came out with a touch-screen, which of course changed everything as the entire face of the phone could be used as a screen. Flexible screens for phones are nevertheless being researched all the time, as shown in a frame of a video in Figure 25 of a Samsung prototype phone, where the screen can be bent all the way around without breaking it or disturbing the image.

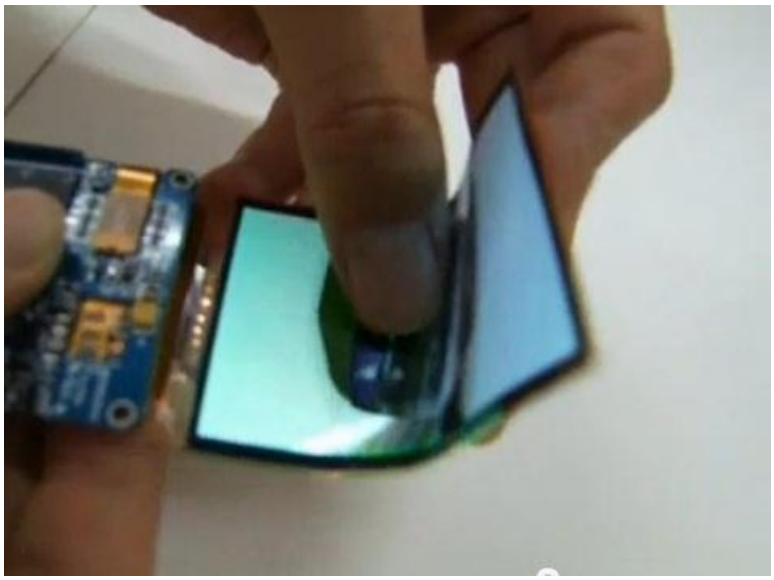

Figure 25. Samsung's prototype mobile phone with a very flexible display. (Technology-Update.us 2010)

2.9 Sintering, Laminating in Inks in Printed Electronics

In conventional electronics production the process of producing electronics is called a wet process. A wet process involves a complex process involving chemicals and liquids which has high equipment costs. It also produces lots waste and is harmful to the environment. Electronics printing, on the other hand, works by printing a required pattern of metal nanoparticles onto a substrate and after that the product is heated up. (Maekawa et al. 2012, 868)

There are many different inks used in electronics printing in order to produce the actual electronics, but each of them has the main task of conducting electricity. Drying means heating up the substrate with the ink, so that liquids vaporize from the ink and only the conducting parts are left on the substrate in a desired pattern. It might seem like a good idea to print using molten metal, but this is not possible when the substrate is so thin and cannot withstand such high temperatures.

The solution is to make an ink that contains different solvents and nanoparticles (Figure 26) from a highly conductive metal such as silver (Ag). Although metals usually have a very high melting point when they are in bulk format, their melting points decrease significantly when they are in the form of nanoparticles. Because nanoparticles are so small, the ratio between the number of atoms on the surface and in the volume is much higher than normal, and the particles melt at lower temperatures. This is called the size effect of the thermodynamic properties. (Luo et al. 2008, 2359)

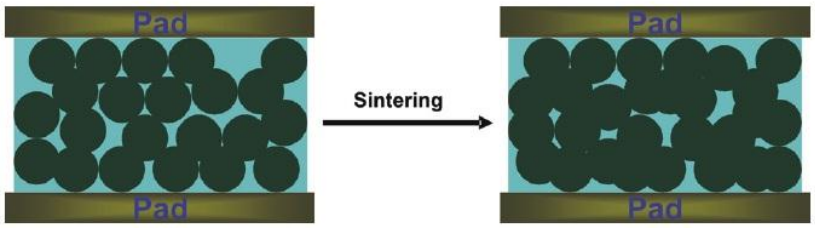

Figure 26. How nanoparticles form into a conductor in sintering conductive adhesive filler. (Zhang & Wong 2009, 150)

New inks are constantly being researched and they will have a significant influence on printed electronics technology. The goal is to make an ink that can be dried at a low temperature, and the product should have a low electrical resistivity. Major developments in these inks could revolutionize the printed electronics industry. (Luo et al. 2008, 2359) The properties of silver inks properties are dependent on the particle size, shape, density and the resin system. The solids content can be controlled by adding isopropyl alcohol and other appropriate solvents to the given ink. (Hrehorova et al. 2011, 318)

Electronic printing could also use nanotubes made of carbon. These tubes are very small, and in research conducted by Ryu et al. (2008, 21), a transistor array made from them was only 50 nm thick. The nanotubes are flexible and can be printed on virtually any surface, such as polymers, glass, silicon and fabrics (Figure 27). Also these nanotube-transistors can be made transparent, so they could be perfect for manufacturing flexible and transparent displays.

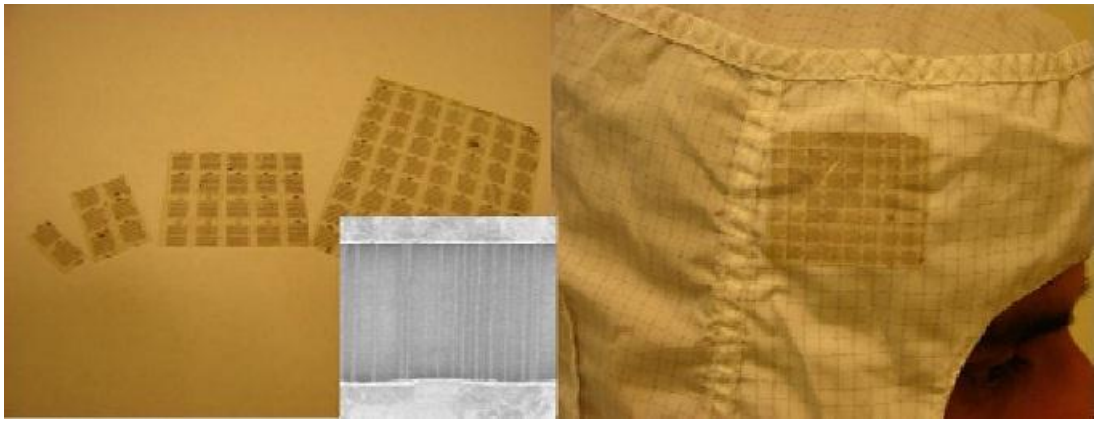

Figure 27. Electronic textile (right side) made from nanotube transistors (left side). (Ryu et al. 2008, 22)

2.10 Register Control in a Roll-to-Roll System

As discussed earlier, the roll-to-roll printer usually contains several separate printing sections in order to make a multilayer print. These prints must be set precisely in the correct position on top of each other. However, the temperature effects and motors pulling the substrate can cause the substrate to be set in an incorrect position. Register control is a stabilising system that prevents this.

If the registers are not in their correct places, a register error occurs. The register marks are actually small marks made of ink and layered on top of each other (Figure 28). According to Choi et al. (2010, 869) the register marks could, for example, be a triangle in the first printing unit and a circle in the second. This way you can measure the distance of the triangle outside the circle to see the register error.

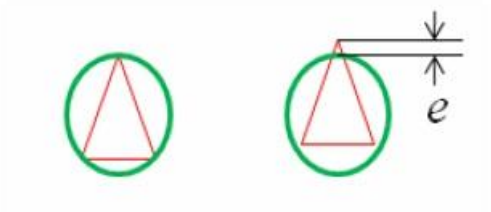

Figure 28. A simple way to measure the register error in a multi-layered printing machine. (Choi et al. 2010, 869)

The actual marks are printed with the inks used to print the electronics, and the marks are measured using high precision cameras.

2.10.1 Compensation-Roll-Type Register Control

There are two ways to control the register. First is the compensation-roll-type register control (Figure 29). In the compensation type register control, there are separate spans in between the printers where three rolls, one of which is able to move up and down, create a system that can alternate the length of the compensation span. Changing the length of the span can correct any register errors created in the previous span by motors

or temperature. Also, the engines of separate rolls are usually powered by a main motor and a main shaft that delivers exactly same speeds to the rolls. (Kang 2000, 3) Moreover, the tension of the substrate can be measured with a roll like this. Sometimes the compensation roll is called a dancer. (Kang 2000, 31)

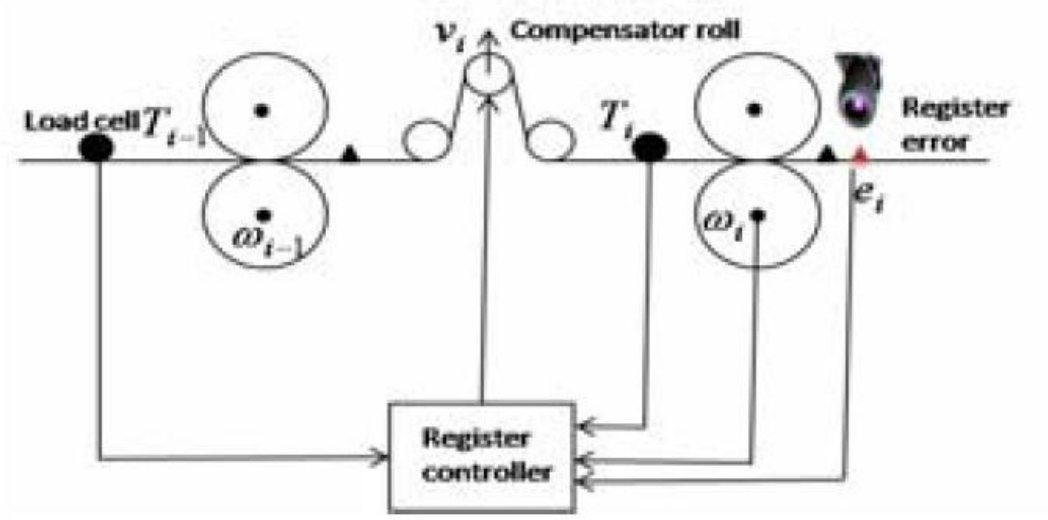

Figure 29. Diagram of the compensation roll register control. (Choi et al. 2010, 870)

2.10.2 **Shaftless-Type Register Control**

The second type of register control is the shaftless-type (Figure 30). It is a much simpler technology in which the rolls are driven by separate motors and a main controller. This way the rolls can move separately at different speeds according to the needs of the controller to keep the register in the right position. (Kang 2000, 3)

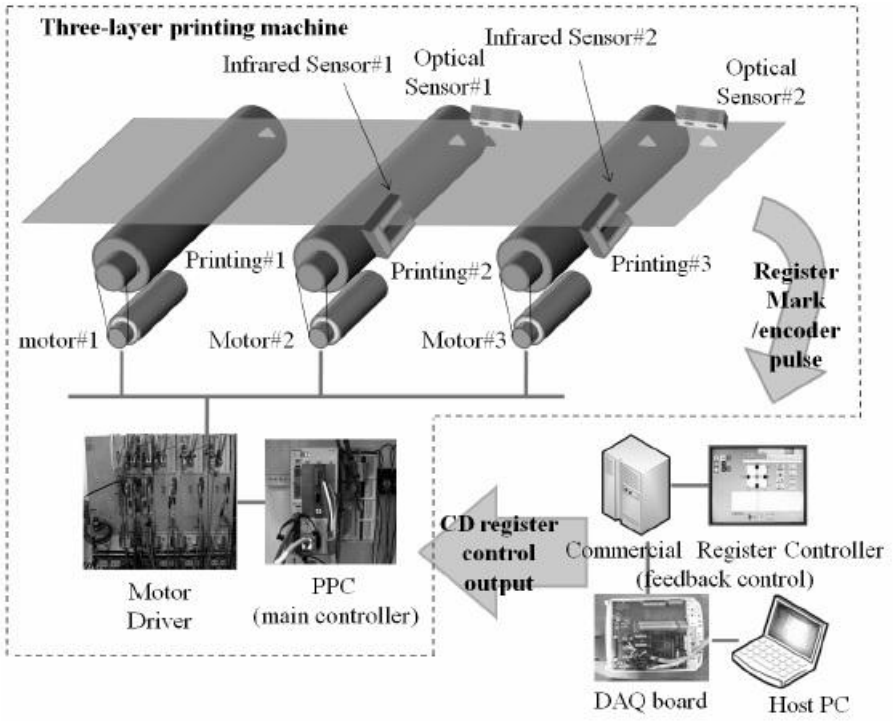

Figure 30. The basic idea behind the shaftless register control. (Kang et al. 2009, 395)

The shaftless system is controlled by adjusting the speed of the substrate, and the compensation system is controlled by adjusting the length of the span between the printing rolls. The shaftless system is more common because it is simpler to build. (Kang 2000, 4)

2.11 Experimental Analysis and Design

In order to design the experiments for determining the effect of the thermal expansion of the web on the tension, we should examine some methods of design and analysis of experiments.

Firstly, in order to make an experiment we must beforehand determine the different factors (Figure 31) that influence the process. There is usually an input of something and an output, and during the process the input is influenced by controllable and uncontrollable factors. (Montgomery 2009, 3)

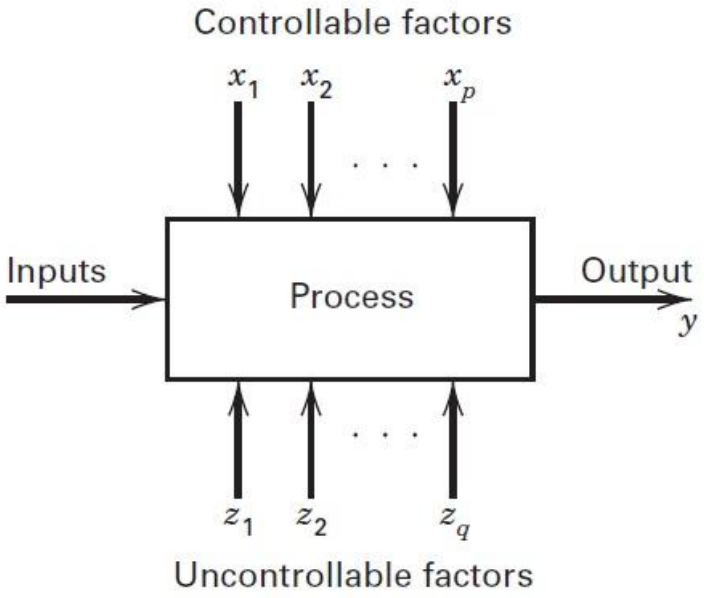

Figure 31. Factors influencing the outcome of the experiment. (Montgomery 2009, 3)

Sometimes there are also factors that are only controllable because of the experiment. What is important is to determine which factors will be examined during the experiment? The idea is to select the ones that have the greatest influence on the output. The knowledge of what those factors are usually comes from the researcher with extensive experience in the field. The more factors are included in the test, the more complicated it is to determine what are the best conditions for producing the optimum

output. For example, if there are two factors that have two different possible input values, we get $2^2 = 4$ different conditions for the initial values. If we have 10 different factors with two different possible inputs, we get 2^{10}=1024 different initial conditions. In order to test this, it might take too much resources and time, so the number of factors has to be reduced to the minimum. (Montgomery 2009, 3-7)

2.11.1 Examples of Different Types of Experiment Design

The style of experiment, in which all the possible initial conditions are explored is called a **factorial experiment**. It is a type of experiment design. An experiment with 2 factors with 2 possible values is called a 2^2 factorial design. If there are too many factors or values involved, all the experiments involved in a factorial experiment cannot be conducted. Then a **fractional factorial design** can be conducted. This way only a proportion of the combinations are explored, in an attempt to determine the most important key influences from the configuration. (Montgomery 2009, 7)

The factorial design of experiments is a sound empirical experiment because it explores the combinatory effects of different factors. Often in popular science the idea of the **one factor-at-a-time approach** is represented as a sound approach to experimenting. Unfortunately, in most cases this is not true. In the one-factor-at-a-time approach, all the different factors are tested separately, and the separate results from the effects of the factors will lead to an idea of which choices to make to produce the best results. The problem is that it ignores the factorial effects of different factors happening together. Often a single factor might not make a change by itself, but only when occurring simultaneously with another factor. Therefore, some factors that might be crucial when combined will be rejected as insignificant in the one-factor-at-a-time approach. (Montgomery 2009, 4)

The **best guess approach** is another easy and quick way to determine the best initial values. The researcher simply makes his best guesses about which values will produce the best yield, and conducts the experiment. This may work in a situation where lots of experiments have already been conducted, or an in-depth knowledge of the system is at

place, but it is a risky approach because only a small number of experiments will be conducted. (Montgomery 2009, 4)

In some situations there might only be two parameters to change, but the area of inputs that produces the best yield is unknown. In this situation, it might be a good starting point to carry out four experiments with two different inputs on both parameters, and create a three-dimensional contour map (Figure 32), with the yield being the third dimension. The first results will give a direction of a better yield, and the subsequent experiments can be carried out with inputs from that direction. This is called a **response surface methodology**. (Montgomery 2009, 10)

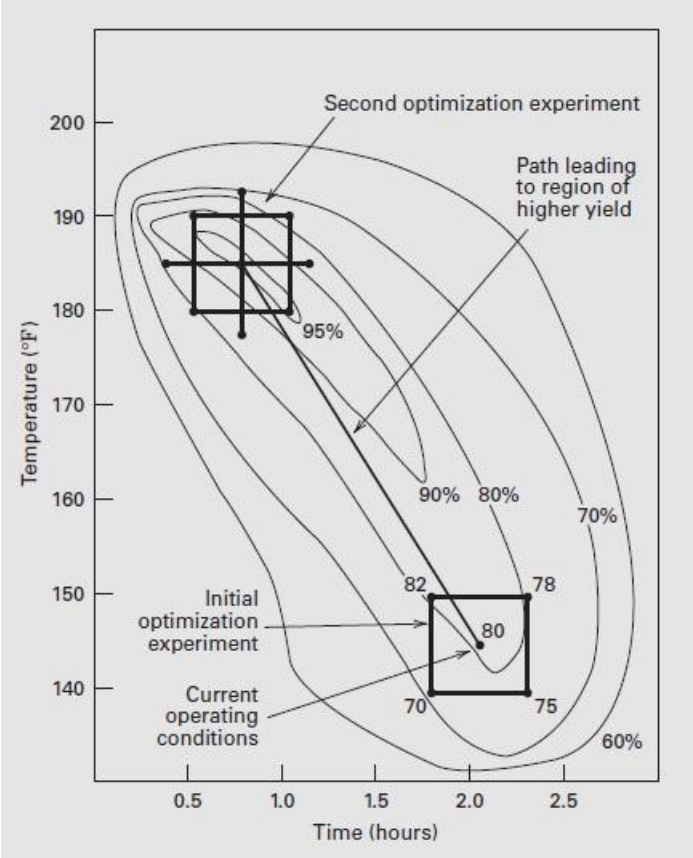

Figure 32. A three dimensional search for the best yield in an experiment. (Montgomery 2009, 10)

This approach is very similar to a one-dimensional problem, where changing one parameter changes the yield and the best input is unknown. In that situation one would simply go in the direction of the best yield.

2.11.2 **Principles of Experiments**

There are three main principles for making experiments statistically proof; randomization, replication and blocking.

True randomization is important because without it the results will be affected too much by the inputs. Randomization should be used when selecting the experimental material and the order of the experimentations. If the materials are selected in order to increase the chance of a certain type of result, the experiments will not be statistically proof, and other scientists carrying out the same experiments will not come to the same conclusions. The order of experiments may also have an effect on the results, so it should also be randomized. (Montgomery 2009, 12)

Replication means that when conducting experiments with different inputs, the different inputs should be replicated. This way, the statistical error can be defined from the difference in the results between the experiments with the same parameters. It should be noticed, though, that repeated measurements are not the same thing as replication. Repeated measurements could be used, for example, to measure the length of the same log three times, or measure the differences in taste of four pies that were baked at the same time. A true replication would be to have two separate logs measured or to have four separate pie-making sessions with the same recipe. All depends of course on the specified differences that the experimenter is looking for. (Montgomery 2009, 12)

Blocking means that experiments are put into different blocks depending on the batches of raw material used. Within one bag of flour, the sizes of the grains are probably similar, whereas compared to another bag they might differ a lot. This can have a considerable effect on the outcome of the pie. When the results of the experiments are put into blocks, they can be considered separately. (Montgomery 2009, 13)

3 THERMAL STRESS MODEL BUILDING AND VERIFICATION

3.1 Experiment System Configuration

First let us look at the roll-to-roll printing machine configuration used at KU-FDRC from Figure 33.

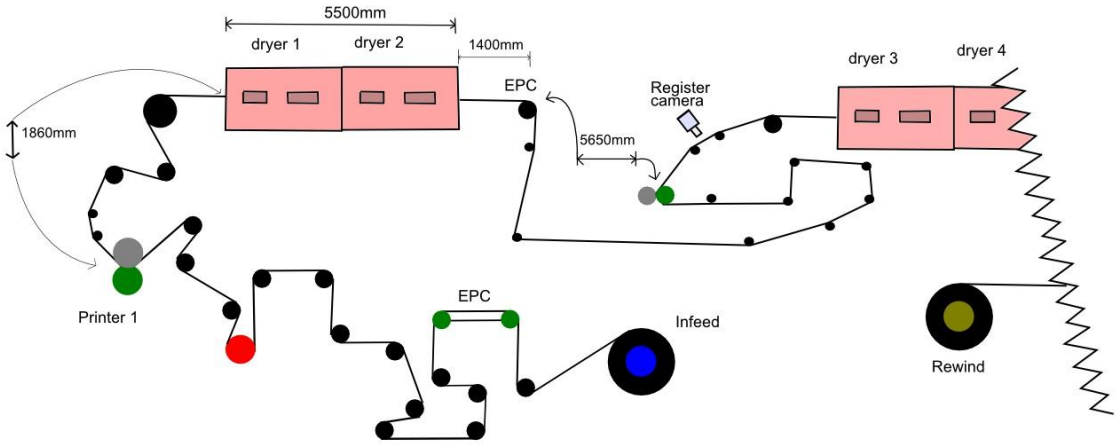

Figure 33. Configuration of the web in the measured area from the infeed to the second printing unit.

The roll-to-roll web starts from the big cylinder (circle) in the middle of the picture. From there it travels left through the EPC (edge position controller). Next is a dancer, which controls the MD position and therefore the tension of the web. After that the heating roll prepares the web to be more flexible for printing. Then the gravure roll makes the print. There are several load cells in the system which measure the tension of the web at different stages. After the load cell, the web travels straight into the dryer (also known as the heater, Figure 34) which sinters the patterned ink onto the web.

Figure 34. Printer dryers one and two, with the in-feed mechanism below.

The dryers work by hot air. The web travels through two dryers and comes out onto an EPC. After that, the web goes through two air flotation rolls (Figure 35), where the web does not touch the roll but is pushed out by air in order to avoid scratches to the printed material. Finally the web moves on to the register mark camera and then on to the second dryer, which has a similar mechanism.

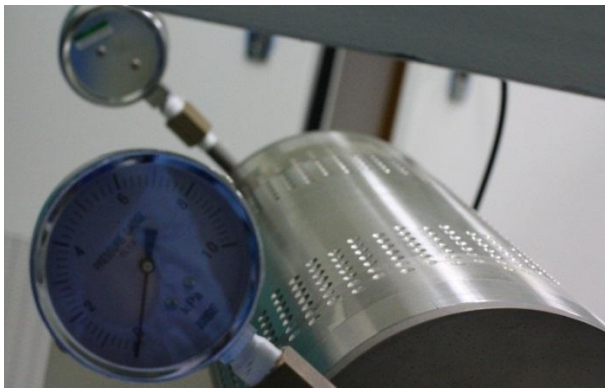

Figure 35. Air-flotation cylinder after the dryer.

It should be noted that during these experiments no tension control system was used. The dancer was not used to change the tension, and the speed of the driving engines was kept static. This means that the system is working statically, and the results of tension variations are only caused by differences in the heat, so we can use the results to derive a mathematical model of the effect of temperatures on the moving substrate.

3.2 Measurement Devices

In the machine, between the dryers, the web register marks are either monitored using a camera or scanned with a line-scanner.

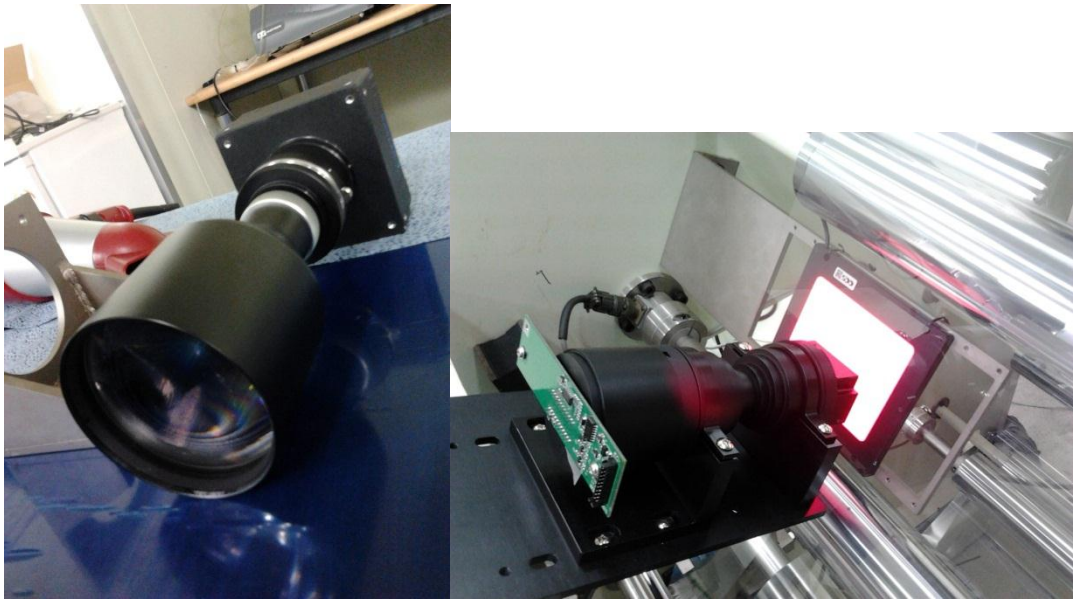

Figure 36. A register mark camera (left) and a line-scanner at work (right) at the KU-FDRC in Seoul, South Korea.

The camera on the left in Figure 36 is a Basler A402k, with a field of view of 50x36.7 mm^2, shooting at a pixel size of 12 µm / pixel and 24 frames per second. The lens in the picture can only make out 20 µm / pixel. In the picture it is not installed onto the printer system.

In Figure 36 on the right you can see the line-scanner at work. The web is in fact there, though it is difficult to recognize because it is transparent. The camera or line-scanner takes pictures of the web and the register marks and feeds the information digitally to a computer with a customised program that determines the register error of the web.

The heater uses hot air to sinter the printed ink, and it is controlled by a proportional-integral-derivative (PID) controller. When a setpoint is changed in the PID controller,

the temperature rises towards the setpoint and then starts to oscillate around that temperature. The size and length of the temperature oscillation depends on how the PID controller is tuned.

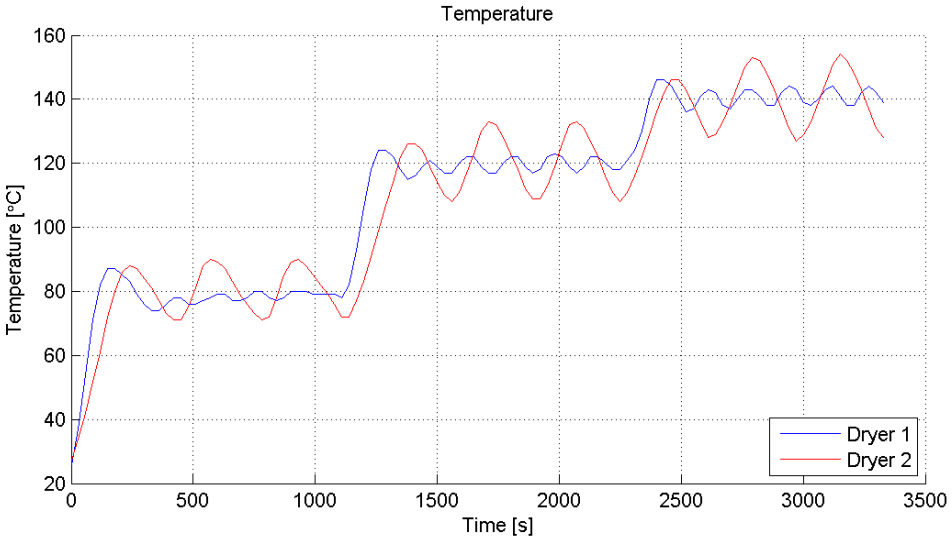

Figure 37. Temperature fluctuation in the first and second dryer. (KU-VTT 2012)

From Figure 37 it can be seen that the first dryer's PID controller is tuned precisely, since the temperature fluctuation is much smaller than in the second dryer. The second dryer has a much larger temperature fluctuation, and the PID controller should be retuned.

Temperature is one of the main factors causing tension fluctuations in the web. The load cell in the system has a pressure measurement device that feeds a voltage to a National Instruments Data Acquisition board (DAQ) that turns the analogue information of voltage into a digital input into the computer. The computer receives the data, it is processed with an equation and the Matlab program produces the results in Newtons.

3.3 Substrate Property Testing Results from the Korean Polymer Testing & Research Institute

In order to produce a mathematical model of the web at hand, we need precise information on the properties of the substrate at different temperatures, especially on the elastic modulus and thermal expansion coefficient. Tests were ordered from the Korean Polymer Testing & Research Institute (KOPTRI).

3.3.1 PET Elastic Modulus in Different Temperatures

Tests for the PET's elastic modulus consisted of stretching a piece of PET in different temperatures. The Figure 38 shows the expansion of a strip of PET at 120 ºC in relation to the force required to stretch it.

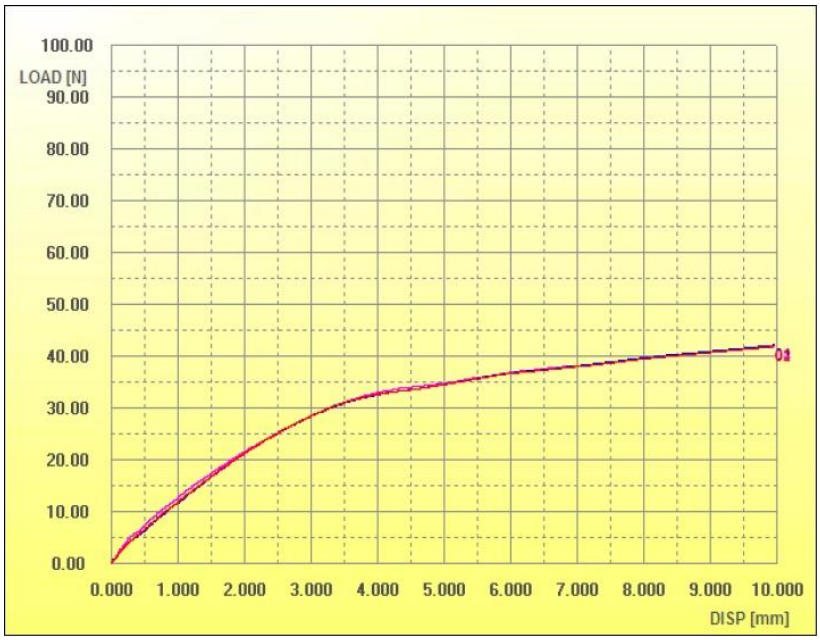

Figure 38. Force required for stretching a 100 mm strip of PET film. (KU-VTT 2012)

As you can see from the figure, at the beginning the plastic is less elastic, and as it stretches more it takes less force per strain to stretch the polymer. In this test the breaking point was not a desired result, so the stretching ended at 10 mm of disposition. The original strip of PET was 100 mm long. The tests were replicated, and there are

several curves in the figure, even though it is difficult to see this. The lower temperatures showed a stronger resistance at the beginning of the stretch, which was expected. The tests were carried out at 50, 80, 100, 120 and 150 ºC. From these data a mathematical model for the elastic modulus of PET (Figure 39) was produced by James Seong at KU-FDRC using Matlab.

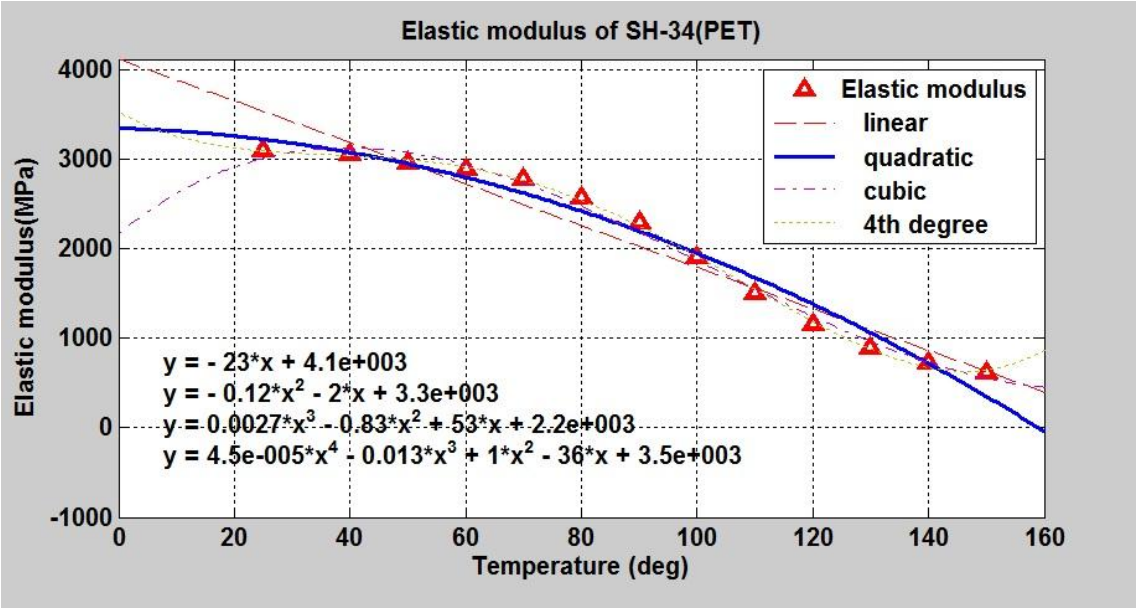

Figure 39. Mathematical model for the elastic modulus of PET considering temperature. (KU-VTT 2012)

The model behaves as predicted. The elastic modulus declines as the temperature rises, until reaching a high temperature, where the PET's structure is starting to change.

3.3.2 PET Thermal Expansion Coefficient

The thermal expansion coefficient is difficult to find from literature, supposedly because it might change with the various different PET crystallisation forms and structures. Tests were run (Figure 40) and a short piece of PET, the size of 5.22 mm expanded in heat.

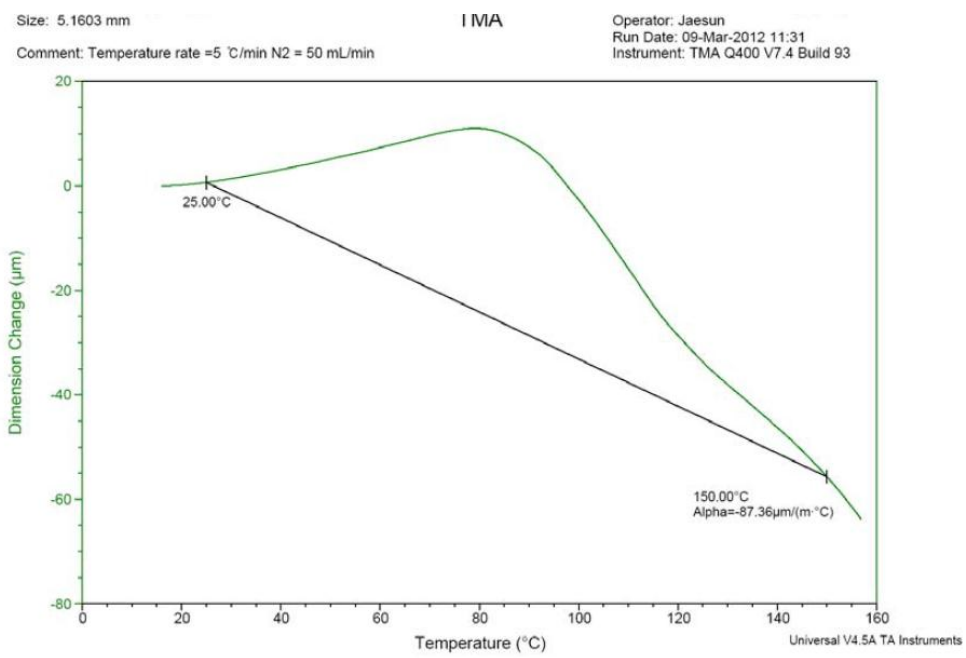

Figure 40. Expansion of PET film at different temperatures. (KU-VTT 2012)

As we can see from the graph, the film expands until 80 ºC, after which it starts to shrink rapidly. To produce an extensive mathematical model of the roll-to-roll machine we also need to make a mathematical model for the thermal expansion.

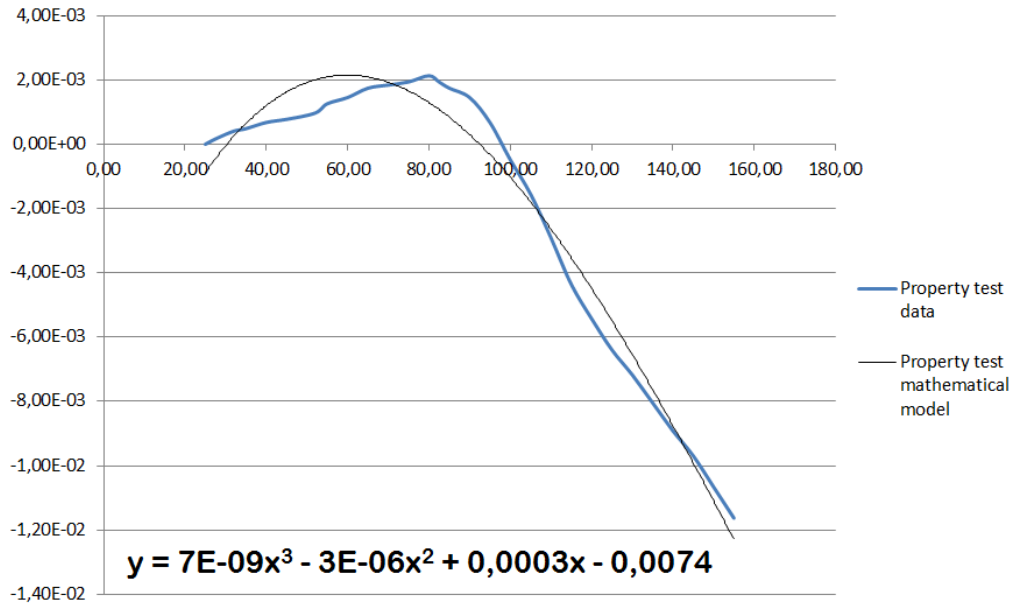

Figure 41. The third order mathematical formula of thermal coefficient.

The model in Figure 41 is close to the real data and can be used to estimate the effect of thermal expansion and shrinkage in the web.

3.4 Problem and Hypothesis of Web Tension Fluctuation

The span between the two rolls that are heated actually has three thermally different parts. The first part is after the load cell and before the heater. The second is in the heater and the third one is the part after the heater. These parts are at different temperatures, and as discussed earlier, the PET film first expands and later shrinks as the temperature rises.

From Figure 37 we can see that there is a major oscillation in the tension (occurring about 3 times per degree change) that is clearly caused by temperature fluctuation in the dryer oven, as there the temperature fluctuation is similar. There are other shorter frequencies in the tension variation that are probably caused by other things like measurement noise or differences in the engine speeds. These interferences were being studied simultaneously with this work at the KU-VTT Joint Research Center.

One should notice that the tension is decreased when heated, which is to be expected, but then it begins to increase again. Tension control was not used in the experiment, so it is not because of this. Also, we assume that it is not due to the polymer changing its form or substrate movement, but only because in the experiment discussed previously the tension had not risen to its steady state before the heat was turned on, and the machinery has a tendency to raise the tension slowly to its steady state.

Assumptions: Heat increase creates a tension drop in the system because of increased elasticity and heat expansion.

Problem: The tension changes in the span according to temperature, tension in the upstream of the web and the speeds of the rolls. The change in the temperature changes the elasticity of the substrate and it also expands or shrinks the substrate at different temperatures. We should determine what the scales of these effects are in relation to each other.

Initial observations: As discussed previously, PET expands thermally until 80 ºC and then plummets sharply into shrinkage. When the web is heated to 80 ºC, it expands the

most, causing the largest dip in the tension graph. If heated above 80 ºC to 120 and 140 ºC, PET will shrink instead of expanding, and the shrinkage should cause a rise in the tension instead of lowering drop. Considering the elastic modulus, which decreases as the temperature rises, the smallest change is actually from 24 - 80 ºC, while from 80 – 120 ºC and 120 – 140 ºC the change is considerably bigger.

24 – 80 ºC: Tension decreases 50%. The web expands about 2 mm / m, but the elastic modulus decreases by 20%.

80 – 120 ºC: Tension decreases 40%. The web shrinks 6 mm / m and the elastic modulus decreases by 50%.

120 – 140 ºC: Tension decreases 20%. The web shrinks 4 mm / m and the elastic modulus decreases by nearly 50%.

Looking at this data, we can say that **at 24 – 80 ºC** the drop in the tension is the greatest because the web expands and the elastic modulus is reduced, both of which decrease the tension. At **80 – 120 ºC** and **120 – 140 ºC,** the web shrinks, which causes a tension increase and the elastic modulus is reduced a lot which causes tension decrease. This means that they cancel a part of each other out. Also, it should be noted that the reduction in the elastic modulus also lowers the effect of the force of the thermal shrinkage. In the 24 – 80 ºC section a change of 1 mm / m in expansion will have a three times bigger effect than at 120 – 140 ºC**.**

Hypothesis: The thermal expansion and shrinkage of the web and the change in the elastic modulus have a similar scale of effect on the force measured by the load cell of the web in the dryer.

By calculations and simulation we can predict how big the actual thermal expansion and shrinking effect will be compared to the effect of the decreasing elastic modulus and, of course, compared to the effects of the upstream tension and speed differences in the rolls.

3.5 Mathematical Model of the Moving Web

To start with, we need to examine the theory of stress induced in the substrate by the velocity differences of the rolls and the strain in the upstream roll. Let us take a look at a control volume from the studies of Lee et al. (2009, 1097)

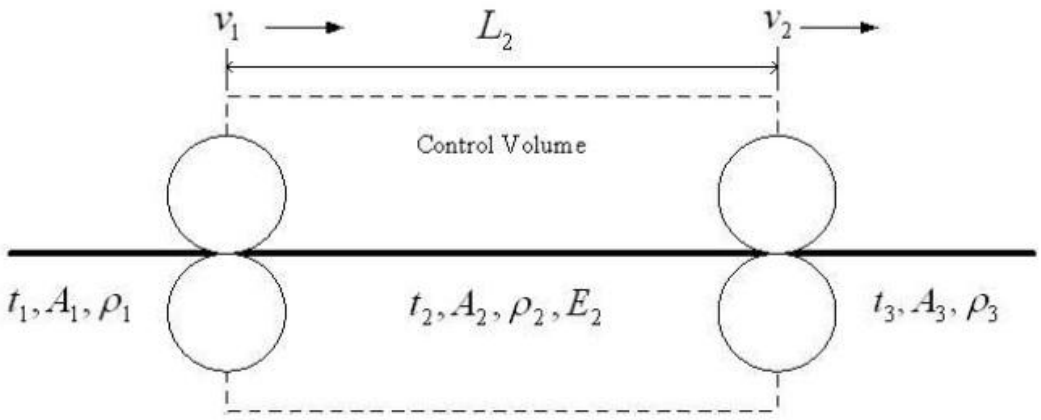

Figure 42. Control volume of roll-to-roll substrate between two rolls. (Lee et al. 2009, 1097)

In Figure 42 we can see the symbols: t = tension, A = cross sectional area, ρ = density and L for length. The V_1 and V_2 represent the speeds of the rolls that are pulling the substrate.

Now we can formulate the mass conservation of the control volume. (Shin 1991, 22)

There are some assumptions that have to be made:

(1) The rollers pull the substrate perfectly and are not able to slip.
(2) The contact region length to the roller is insignificant for the substrates tension.
(3) The web is perfectly elastic.
(4) The material of the substrate is isotropic.

(5) The substrate is isotropic in its defined areas. (Later there will be more than one)
(6) The substrate is uniform i.e. has the same dimensions everywhere.
(7) There is no mass transfer between the web material and rollers.
(8) The thickness of the substrate is very small compared to the radius of the rollers.
(9) The substrate only stretches in its machine direction (along its length).
(10) The strain in the web is very small, not even close to unity.

Notice that the substrate's properties are able to change as a result of temperature change. This means that when the substrate's temperature rises, it becomes looser, its Young's modulus becomes smaller and it will expand. This will be taken into consideration in the mathematical simulation of the substrate.

3.5.1 **Mathematical Model Considering Velocities and Tensions**

The following formulation is from Shin's (1991, 21-26) doctoral thesis, adapted to the needs of this simulation.

Let us also consider that in the previous equation the web was not stretched. The following equation describes the stretching of the substrate in its machine direction. Let us assume that the substrate will not stretch in its other directions.

$$dx = (1 + \varepsilon_x)\, dx_u \qquad (5)$$

The strain on the substrate is ε_x, dx_u is the infinitesimal element that is considered to be stretching and dx is the actual stretched length of the infinitesimal element.

Next let us consider the weight of the stretched infinitesimal element:

$$dm = \rho\, d\, h\, dx = \rho_u\, d_u\, h_u\, dx \qquad (6)$$

The lower index u stands for the unstretched elements. If we combine these equations we get the following equations:

$$\frac{\rho\ d\ h}{\rho_u d_u h_u} = \frac{dx_u}{dx} = \frac{dx_u}{(1+\varepsilon_x)dx_u} = \frac{1}{1+\varepsilon_x} \tag{7}$$

And because A = d × h and $A_u = d_u \times h_u$,

$$\frac{\rho(x,t)A(x,t)}{\rho_u(x,t)A_u(x,t)} = \frac{1}{1+\varepsilon_x(x,t)} \tag{8}$$

We can also leave out the x from the ε_x because we assume that the other directions are not going to stretch.

Now by combining the mass conservation and this last equation we get:

$$\frac{d}{dt}\left[\int_0^L \frac{\rho_u(x,t\ )A_u(x,t)}{1+\varepsilon_2(x,t)}dx\right] = \frac{\rho_{1u}(x,t)A_{1u}(x,t)v_1(t)}{1+\varepsilon_1(x,t)} - \frac{\rho_{2u}(x,t)A_{2u}(x,t)v_2(t)}{1+\varepsilon_2(x,t)} \tag{9}$$

Now from the assumptions that the stretching across the substrate will be equal at any given time and the cross sectional area does not change, we can divide the density and cross directional area out of the equation:

$$\frac{d}{dt}\left[\int_0^L \frac{1}{1+\varepsilon_2(x,t)}dx\right] = \frac{v_1(t)}{1+\varepsilon_1(x,t)} - \frac{v_2(t)}{1+\varepsilon_2(x,t)} \tag{10}$$

And by the assumption that the strain is equal at every point across one span, we can write the equation:

$$\frac{d}{dt}\left[\int_0^L \frac{1}{1+\varepsilon_2(t)}dx\right] = \frac{v_1(t)}{1+\varepsilon_1(t)} - \frac{v_2(t)}{1+\varepsilon_2(t)} \tag{11}$$

By the assumption that the strain is very small, we can make the following assumption:

$$\frac{1}{1+\varepsilon} \cong 1-\varepsilon \tag{12}$$

When combining the last two equations we get:

$$L\frac{d}{dt}[1-\varepsilon_2(t)] = [1-\varepsilon_1(t)]\,v_1(t) - [1-\varepsilon_2(t)]v_2(t) \tag{13}$$

$$L\frac{d}{dt}[\varepsilon_2(t)] = -v_1(t) + v_2(t) + \varepsilon_1(t)v_1(t) - \varepsilon_2(t)v_2(t) \quad (14)$$

This equation is still not linear; the variables are multiplied by each other, so it cannot be simulated. It can be made into a linear equation by a perturbation method.

Let us consider $\in = \varepsilon - \varepsilon_0$ and $V \equiv v - v_0$. (15)

Also let us write the last given equation into the initial steady state where the difference in the length is still zero.

$$0 = -v_{10} + v_{20} + \varepsilon_{10}v_{10} - \varepsilon_{20}v_{20} \quad (16)$$

After that, by combining the three last equations and dropping second order terms we get:

$$\frac{d}{dt}[\in_2(t)] = -\frac{v_{20}}{L}\in_2(t) + \frac{v_{10}}{L}\in_1(t) - \frac{[1-\varepsilon_{10}]}{L}V_1(t) + \frac{[1-\varepsilon_{20}]}{L}V_2(t) \quad (17)$$

Which can be simplified by the assumption that ε_{10} and ε_{20} are very small. That gives us a linear equation:

$$\frac{d}{dt}[\in_2(t)] = -\frac{v_{20}}{L}\in_2(t) + \frac{v_{10}}{L}\in_1(t) - \frac{V_1(t)}{L} + \frac{V_2(t)}{L} \quad (18)$$

This equation shows the linear connection between the strain on the web and the velocities of the rolls and the tension before the control span. As can be seen here, if the velocities of the rolls are the same, they are variables in the equation that cancel each other out. Then again, if the velocity of the first roll is larger than the second one, the substrate will flop, and as can also be seen in the equation it will lessen the strain on the span. Also, if the strain is already high in the upstream at $\in_1$ it will make the $\in_2$ bigger as well. This is understandable because, if you imagine that the substrate was already being pulled in the previous section, it would also cause the substrate to be strained in the next section. Now if we add Hooke's law of force deformation relation:

$$T = AE\in \quad (19)$$

T is the tensile force of the substrate and E is Young's modulus, we can combine equation 18 and 19 this way: (Shin 1991, 21-26)

$$\frac{d}{dt}[T_2(t)] = -\frac{v_{20}}{L}T_2(t)+\frac{v_{10}}{L}T_1(t) + \frac{AE}{L}[V_2(t) - (V_1(t)] \quad (20)$$

3.5.2 **Mathematical Model Considering Temperature Changes**

Now we have the formula for the strain on the span in respect of the speeds of the rolls and the strain on the previous span. Yet, the change in temperature can also induce strain on the substrate, as materials usually expand when heated. Because strain is simply the relation of the change in the length of the span to the span's original length, we get the thermal strain as follows, while remembering that we will assume that the strain is induced only in the machine direction e.g. the direction the substrate is moving:

$$\epsilon_x^t = \alpha \times \theta_T \quad (21)$$

The coefficient of thermal expansion is α and θ is the difference in temperature in the given span.

Now again we can leave the subscript marking x out of the ϵ^t to make it more simple, since we are only interested in the stress in one dimension. Also to combine the thermal and elastic strain into the total strain, we simply add them together:

$$\in_T = \in^e + \in^t \quad (22)$$

To make this into a force relation we need to combine the force relation equation (19) with the tension formulas:

$$F_e = AE \in^e \quad (23)$$

and

$$F_t = AE\, \alpha\theta_T \quad (24)$$

And therefore the full stress force implemented from the elastic and the thermal strain of the substrate in the span comes from:

$$F = AE(\in^{e} + \alpha\theta_T) \quad (25)$$

The span is completely uniform as regards temperature.

All previous equations were from Shin (1991, 21-26), and from here forward the equations have been formulated and modified to a single span with three parts from the work of Lee et al. (2010, 1099) by the author during the work at KU-FDRC in Seoul South Korea. In the studies of Lee et al. (2010), the span with the heater is considered to have a thermal gradient. In the laboratory we do not have the means to determine the temperature gradient of the web, so a simpler approach has been taken.

The problem with our previous equations has been that the actual span in the system is more complicated than one isothermal web. The simulations have not been accurate enough. Here is a sketch of the actual system in Figure 43:

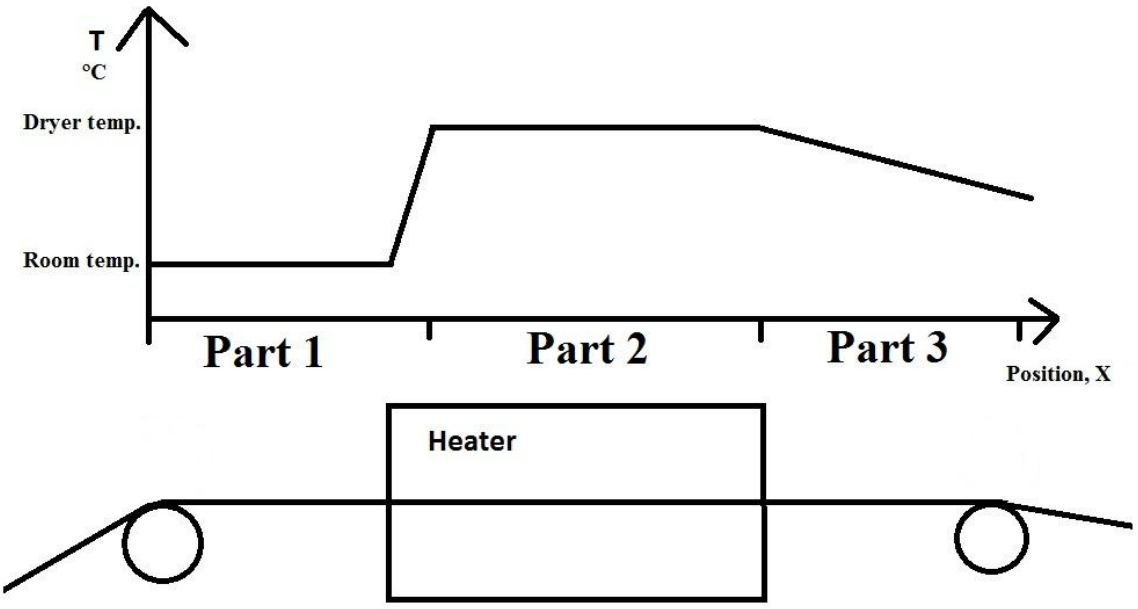

Figure 43. Approximation of the assumed temperatures in the heating span.

There is one span, but three distinct parts to it. The first part stays relatively stable and at room temperature. The second part experiences a rapid temperature rise in the oven, and is kept at the desired temperature until it comes out. The third part is the most interesting, where the temperature starts to drop as the web cools off at room temperature.

Let us make some assumptions about the heat profile in the machine:

(1) The temperature in the first part of the span is the same as room temperature.
(2) The second part of the span will be isothermal, and the temperature will be the same as the heater temperature.
(3) The temperature will drop linearly in the third part of the span due to laminar convection.
(4) The Young's modulus will change according to temperature in a non-linear fashion depending on the substrate material.
(5) The thermal expansion coefficient will change according to temperature in a non-linear fashion depending on the substrate material.

With these parameters we will be able to model a more accurate calculation of the total tension in the heater span. First of all let us look at the thermal expansion part of the force equation, as it is the simplest one.

$$\in^{t} = \in (\bar{T}_i) \tag{26}$$

$\in (\bar{T}_i)$ means the function of the thermal expansion fitted from the expansion property test data (ch. 3.4.2). This function only outputs the change in length from the room temperature, so to get the change in one part, we could mark it as an integral of the derivative which is the expansion coefficient equation.

$$\in_i^t = \int_a^b \propto (\bar{T}_i) \tag{27}$$

Next we should be able to make an equation for the thermal expansion force considering the three distinct parts:

$$F_T = A \times \sum_{i=1}^{3} E(\bar{T}_i) \in_i^t (\bar{T}_i) \times \frac{L_i}{L} \quad (28)$$

$E(\bar{T}_i)$ is the function of Young's modulus in the average temperature in part "i" of the web, $\in_i^t (\bar{T}_i)$ is as discussed before and L_i, being the length of the part where this expansion is in effect. In that the expansion only happens in that part, we must calculate all the parts together in a weighted average. This way we get the separate effects of the expansion in different parts summed up.

3.5.3 **Mathematical Model Combining the Elastic and Heat Effects**

Now, in order to combine the thermal tension formula and the elastic tension formula, we need to change the tension in the current span stress $\in_2$ to an equivalent $\in_{2eq}$, which includes the elastic and the thermal tension in that span. The following modulation of the function is taken from the studies of Lee et al. (2010, 1098-1099) with slight modifications.

$$\in_{2eq} = \in_e + \in_t \quad (29)$$

We can insert it into the equation 10:

$$L\frac{d}{dt}[\varepsilon_2(t)] = -v_1(t) + v_2(t) + \varepsilon_1(t)v_1(t) - \varepsilon_{2eq}(t)v_2(t) \quad (30)$$

And then by opening up the $\in_{2eq}$ we get:

$$L\frac{d}{dt}[\varepsilon_2(t)] = -v_1(t) + v_2(t) + \varepsilon_1(t)v_1(t) - \varepsilon_2(t)v_2(t) + \frac{\in_t}{L}V_{20} \quad (31)$$

And we should also remember Hooke's law. Let us modify it to sum together all the different strains in the three different parts:

$$F = A \times \sum_{i=1}^{3} \left[E_i(t) \times \frac{L_i}{L} \times \in_i^i\right] \quad (32)$$

In this way the strains in each part are added together as a weighted average. When we make the equation more straight forward we get this unlinear equation:

$$\frac{d}{dt}[t_2(t)] = -\frac{v_2(t)}{L}t_2(t) + \frac{v_1(t)}{L} \times t_1(t) + \frac{A \times \sum_{i=1}^{3}\left[E_i(t) \times \frac{L_i}{L}\right]}{L}[v_2(t) - (v_1(t)] - \frac{A \times \sum_{i=1}^{3}\left[E_i(t) \times \frac{L_i}{L} \times \in_i^t\right]}{L} v_2(t) \quad (33)$$

The subscript i stands for the part of the span, either 1, 2 or 3.

This equation is not yet linear, but it can be perturbated into a linear version as in the studies of Lee (2010, 1099). This is the result:

$$\frac{d}{dt}[T_2(t)] = -\frac{v_{20}}{L}T_2(t) + \frac{v_{10}}{L}T_1(t) + \frac{A \times \sum_{i=1}^{3} \bar{E}_{i0}\frac{L_i}{L}}{L}[V_{20}(t) - (V_{10}(t)] - \frac{A \times E_2 \times \in_2^t(t) \times \frac{L_2}{L}}{L} V_{20} \quad (34)$$

The full perturbation can be read in Appendix 1. Unfortunately although the perturbation makes the equation linear, with it, we are unable to accurately calculate the changes in the web. This is because, for example, the elastic modulus E cannot be calculated as a function of time. This is in its turn because multiple variables are not allowed to be multiplied together in a linear equation. Nevertheless the equation 29 is linear in the fact that $t_2(t)$ is not multiplied with another variable, and therefore it can be simulated with Simulink.

Now we have a linear equation, but it is difficult to perceive. For clarity, we can simplify the equation by using some coefficient markings:

$$a = A \times \sum_{i=1}^{3} E_i(t) \times \frac{L_i}{L} \quad (35)$$

$$b = -A \times \sum_{i=1}^{3}\left[E_i(t) \times \in_i^t (\bar{T}_i) \times \frac{L_i}{L}\right] \quad (36)$$

And we get this:

$$\frac{d}{dt}[T_2(t)] = -\frac{v_{20}}{L}T_2(t) + \frac{v_{10}}{L}T_1(t) + \frac{a}{L}[V_2(t) - V_1(t)] + \frac{b \times V_{20}}{L} \quad (37)$$

3.5.4 Thermal Model of the Span after the Heater

In order to simulate the heat drop after the heater, we can make an estimation using heat transfer equations from the book *Fundamentals of heat and mass transfer* (Incropera et al. 2006).

First of all, the overall heat transfer coefficient (how many watts the web dissipates per area and temperature degree) can be calculated by acquiring the total convection and radiation coefficients. To calculate the convection coefficient, you need the Reynold's number, the Prandtl's number, and therefore the Nusselt's number, which then equates to the heat transfer coefficient of the surface. Because of the thinness of the film, let us assume that the film is isothermic, so the conduction inside it will be left out of the calculations.

$$\mathrm{Re_x} = \frac{\rho \mathrm{u}_\infty \mathrm{x}}{\mu} \tag{38}$$

Where $\mathrm{Re_x}$ is the Reynolds number, ρ is the density of the fluid flowing (in this case the air), $u_\infty$the speed of the fluid, x is the position or the characteristic length (in this case the length of the part of the span we are studying) and μ is the dynamic viscosity of that fluid. The Reynolds number measures how turbulent the flow is. A higher number means more turbulent. A number lower than 5×10 is generally considered to be laminar and above that turbulent. There are different equations for laminar and turbulent flows. (Incropera et al. 2006, 360).

$$\overline{Nu_x} \equiv \frac{\overline{\bar{h}_x x}}{k} = 0.664 Re_x^{1/2} Pr^{1/3} \tag{39}$$

Where Nu is the Nusselt number, $\mathrm{h_x}$ is the heat coefficient of the convection on the surface of the web, and Pr is the Prandtl number which is a measure of viscosity and heat transfer and can be obtained from various tables (Incropera et al. 2006, 410). From these equations, the heat coefficient $\bar{h}_x$ can be determined.

$$\bar{h}_x \equiv \frac{\overline{Nu}_x x}{k} \tag{40}$$

$$\bar{h}_x = \frac{\left(0.664 Re_x^{1/2} Pr^{1/3}\right)^{1/2} \times Pr^{1/3} \times L}{k} \quad (41)$$

Now to get the radiation heat transfer coefficient, we can use the following formula from The Engineering Toolbox (2012):

$$q = \gamma\sigma(T_h^4 - T_c^4) \quad (42)$$

The emissivity of the substrate is γ, σ is the Stefan Boltzmann's constant, T_h is the temperature of the hot surface (substrate) and T_c is air. To get the heat transfer coefficient:

$$q = h_\gamma A \Delta T = \gamma\sigma(T_h^4 - T_c^4)A \quad (43)$$

$$h_\gamma = \frac{\gamma\sigma\left(T_h^4 - T_c^4\right)}{\Delta T} \quad (44)$$

And after this we can combine the heat coefficients:

$$h = \bar{h}_x + h_\gamma = \frac{\left(0.664 Re_x^{1/2} Pr^{1/3}\right)^{1/2} \times Pr^{1/3} \times L}{k} + \frac{\gamma\sigma\left(T_h^4 - T_c^4\right)}{T_h - T_c} \quad (45)$$

Notice that this equation requires a knowledge of T_h which is the temperature on the surface and yet unknown. Therefore this operation is iterative.

Next we need to determine the differential heat equation of the web. This comes from the assumption that the heat in the convection equals the dissipation of heat when the temperature drops in the web. (Incropera et al. 2006, 257)

$$q_{convection} = q_{dissipation} \quad (46)$$

$$-hA_s(T_w - T_\infty) = \rho V c \frac{dT}{dt} \quad (47)$$

And when the above equation is integrated and arranged properly:

$$\frac{\rho Vc}{hA_s}\int_{\theta_i}^{\theta}\frac{dT}{(T-T_\infty)} = -\int_0^t dt \quad (48)$$

$$\frac{\rho Vc}{hA_s} ln\frac{\theta_i}{\theta} = t \quad (49)$$

$$\frac{\theta}{\theta_i} = \frac{T_w - T_\infty}{T_i - T_\infty} = exp\left[-\left(\frac{hA_s}{\rho Vc}\right)t\right] \quad (50)$$

Where θ referes to temperature difference, and the index i, to the initial one, T_∞ is the room temperature, A_s the surface area, V, the volume of the web, c the heat coefficient of the web and t is the time used to dissipate the temperature difference θ. (Incropera et al. 2006, 258) Therefore, we can determine the average surface temperature of the web by solving T_w from the equation 29.

$$T_w = (T_i - T_\infty)exp\left[-\left(\frac{hA_s}{\rho Vc}\right)t\right] + T_\infty \quad (51)$$

To get the average expansion or shrinkage using the mathematical model for that, we can use half the time that the web takes to transfer from the oven to the EPC, which is the first point of contact for the web after the dryer. This way we know on average how much the whole span may have expanded or shrunk.

Therefore, as we know the distance the web travels after the heater, and we know the speed of the web, we can calculate the time the web travels between the heater and the roll, and we can estimate what the temperature will be before it reaches the roll. Using this information, we can then calculate how much the web will shrink before reaching the next roll, and how this will affect the tension of the web.

Of course, it should be noted that the heat transfer calculations only give an approximation to the correct temperatures. The convection coefficients are experienced to have up to 25% of error compared to the real world. (Incropera et al. 2006, 414)

3.6 Experimental Test Run Conditions

The test run was conducted in the Konkuk University Flexible Display Research Center electronics printing laboratory (Figure 44). The laboratory is situated in a cleanroom.

Figure 44. James Seong M.Sc. (on the right) and an employee from the camera manufacturer installing a new line-scanner.

The machinery was turned on and the temperature in the dryer was first kept at 22 ºC. When the tension in the span converged to a steady state, which took 18 minutes, the dryer was turned on. Table 3 represents the experimental temperatures and times spent in those temperatures:

Table 3. Values used during the experiment.

Experimentation Values

Temperature	22 ºC	80 ºC	100 ºC	120 ºC
Time spent	18 min	60 min	60 min	60 min

Web length	500 m
Web speed	0.5 m / min

The dryer works by hot air. The actual temperatures in the dryers vary quite a lot. This temperature fluctuation and PID controller function was explained in Chapter 3.3. The web is about 500 m long and it is run through the machine at a speed of 0.5 m / min.

As mentioned before, the web is made of PET. It is manufactured by a company called SKC, and the model name is SH-34. The web is carried through the system at a speed of 0.5 metres / minute. The PET has not been through any heat treatment, and has the same expansion and elastic properties as presented before in this work. The cylinders that pull the web with the DC (direct current) motors are all set to pull the web at the same speed, and are not controlled by any tension control system.

The configuration of the system can be seen from Figure 33. The system differs from the basic configuration in the part after dryers one and two; the air flotation cylinders are omitted from the system because no printing was performed and they would have influenced the tension of the web too much. The parts after the second printer were not sketched here because they are of no interest in this measurement. Also in a real system with two printers, after the second printing there would be no interest in that part, because the printing has already been performed, and any mistakes are impossible to fix.

The tests were run for 200 minutes and 36 seconds, and data was collected from 4 different load cells in the system. Temperatures from dryers 1 and 2 were logged by hand onto a computer with a time code. The load cell for the dryer span was the most important data for this study. The hand-logged temperature data is clear enough for the thermal expansion experiment, even though data collection through the DAQ would have been more suitable, but it was impossible to accomplish with the schedule and equipment at hand. 2,047 temperature points were logged. Even though the temperature information is not extremely accurate, it should be noted that the temperature on the substrate is most probably always a little different from the temperature in the dryer.

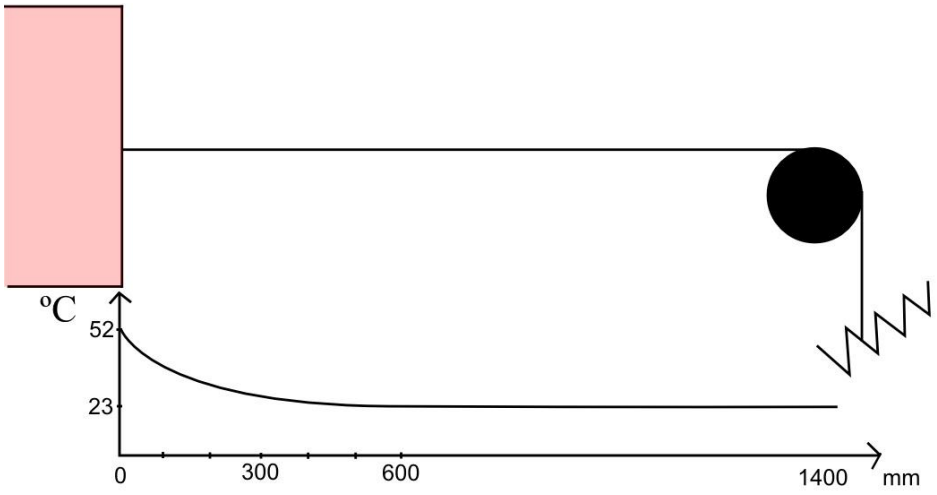

Figure 45. Measured temperature profile after dryer 2 sketched out.

In order to calculate the tension in the dryer span, it was important to calculate and measure the temperatures of the web after the dryers. If the temperature is high, it will have an influence on the elasticity and expansion of the web. In the figure above we can see the first 1.4 metres of the web after the dryer. The part between the dryer and the second printing is 5.56 metres long. Only the first 0.6 metres after the dryer has a slightly higher temperature (Figure 45) so we can assume that it should not influence the tension of the web greatly. It should be noted that the temperature was measured by a hand-operated infrared temperature meter, and it may have a small error because the film is transparent. Even though visible light passes the web, in the IR field of the web it is not as transparent. We can assume that a part of the IR signal is transmitted through and the actual temperature is higher. Still, the web after the dryer seems to be nearly 90% at room temperature, which is enough to say that it should have no significant effect on the overall tension of the span that is 13.01 metres long.

3.7 Matlab/Simulink Simulation of the Substrate's Behaviour

Calculation of the web span in the heater was done with Simulink, which is an expansion to Matlab by The Mathworks Inc. Simulink is often used when differential equations form iterative problems where several factors are changed and influence several different equations. This is also the situation in our problem, as the MD force on the span is affected by the temperature in the span, as well as the speeds of the rolls and tension in the former span. All the different attributes of the span are affected by the temperature at the same time. Simulink can form a timeline where we can input a change at a certain moment, which will then introduce a gradual change in the system.

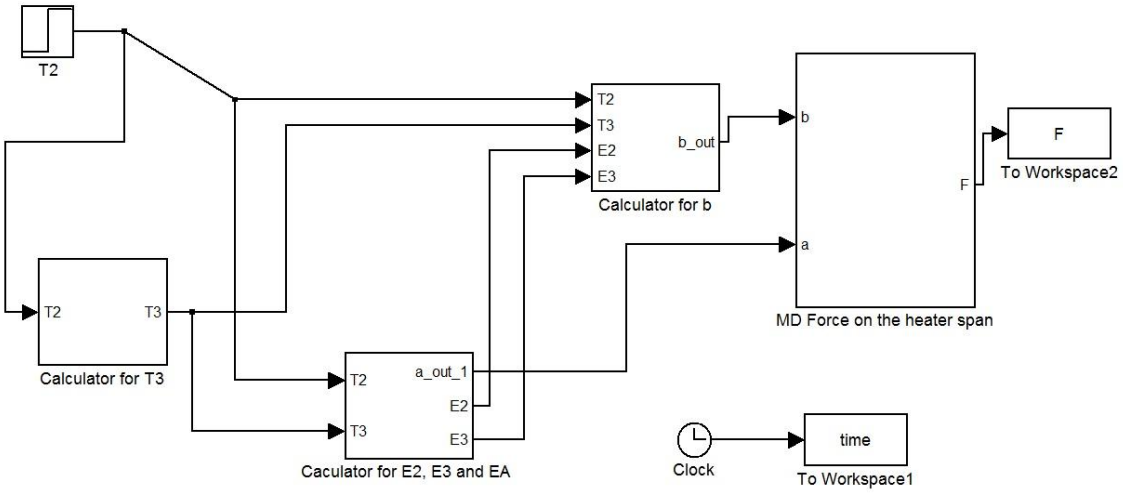

Figure 46. A general picture of the main window of the Simulink simulation of thermal the roll-to-roll web span in the heater according to the formulated equations.

The Figure 46 represents the main configuration of the model. The different parts have windows inside them with formulas and calculations in order finally to calculate the tension force on the web. The time and F is outputted to a workspace which can be printed using Matlab. T2 (temperature in the dryer) on the left can have a step change, which is the change from 23 ºC to 80 ºC when the heater is turned on. This influences all the parameters, as can be seen from the connections.

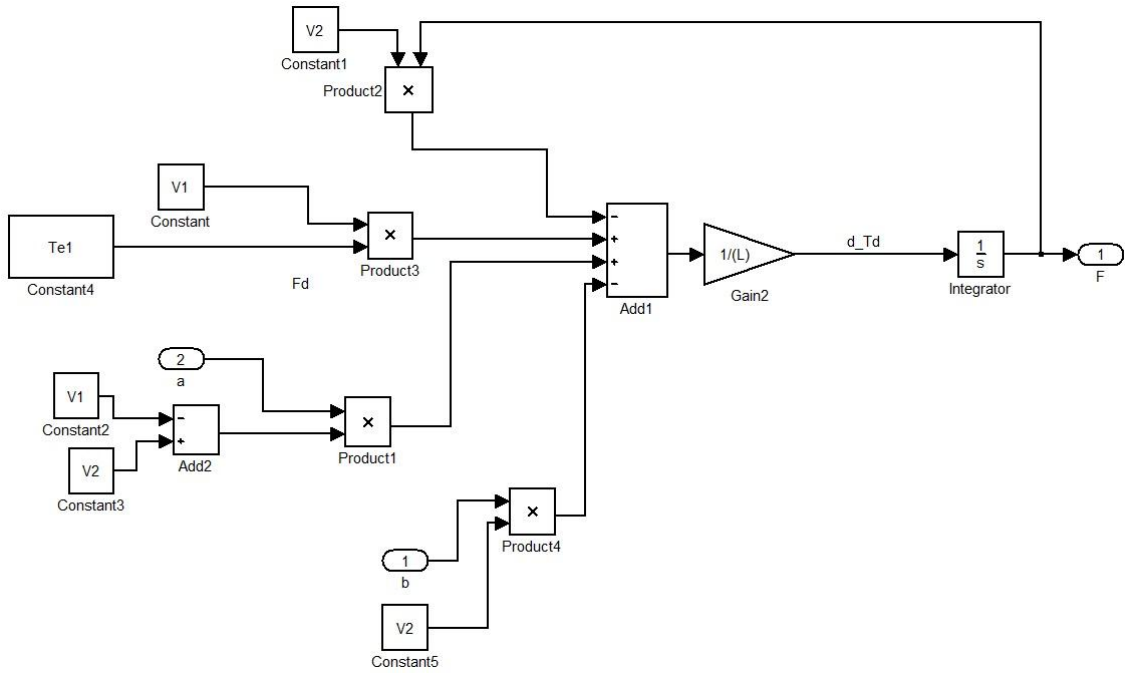

Figure 47. The calculation of the force in the Simulink model.

In Figure 47 one can see the actual integration of the force. The change in the force is calculated on the right by integrating, and the result is used again in the equation. This way we get an iterative response, which can be seen in the final output of the Simulink on force.

4 RESULTS

Previous experiments gave us indications of what kind of a tension behaviour the web has. By studying calculations and formulas from previous studies of webs and thermal expansion, we were able to build a model that should properly predict the tension changes.

4.1 Simulation Results

We simulated the system with the temperature changing from 22 to 80 ºC, with initial tension at 2.25 kgf, the speed of the web at 0.5 m/min, the length of the span at 13.01 m, with the first part 1.86 m, the second (the dryers) 5.5 m and the third 5.65 m. Also for this simulation the expansion of PET was calculated using the trend formula plotted from the KOPTRI test results. We will give all the simulations here enough time to converge to their steady states. Here are the results of the simulation in Figure 48:

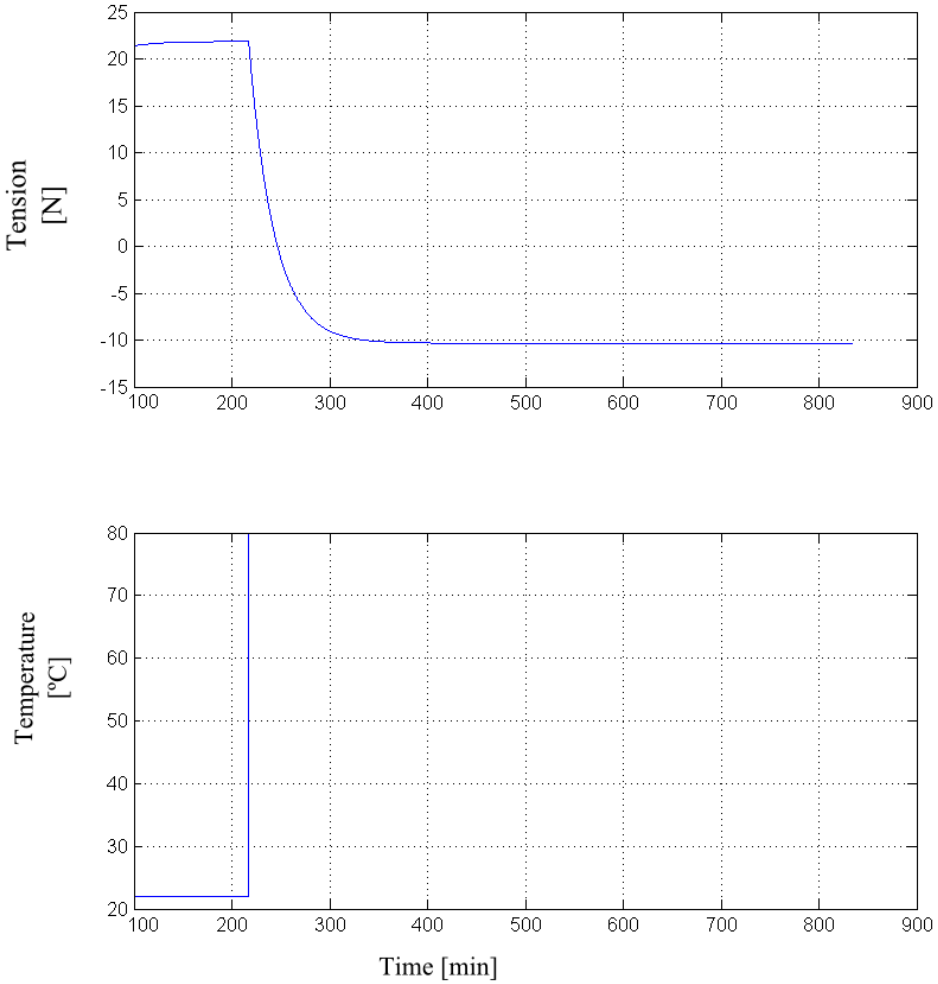

Figure 48. Simulation results of the tension change from the initial tension of 22.5 N to -10 N because of the temperature change of 22 to 80 ºC.

The tension change is -32.5 N. In the experiments the tension change from 24 to 80 ºC was only 12 N at most (Figure 48). This suggests that the real-life system is more complicated and is influence by something that is unknown in the simulation.

The temperature changes from 22 to 80 ºC, 100 and to 120 ºC were simulated with the same properties:

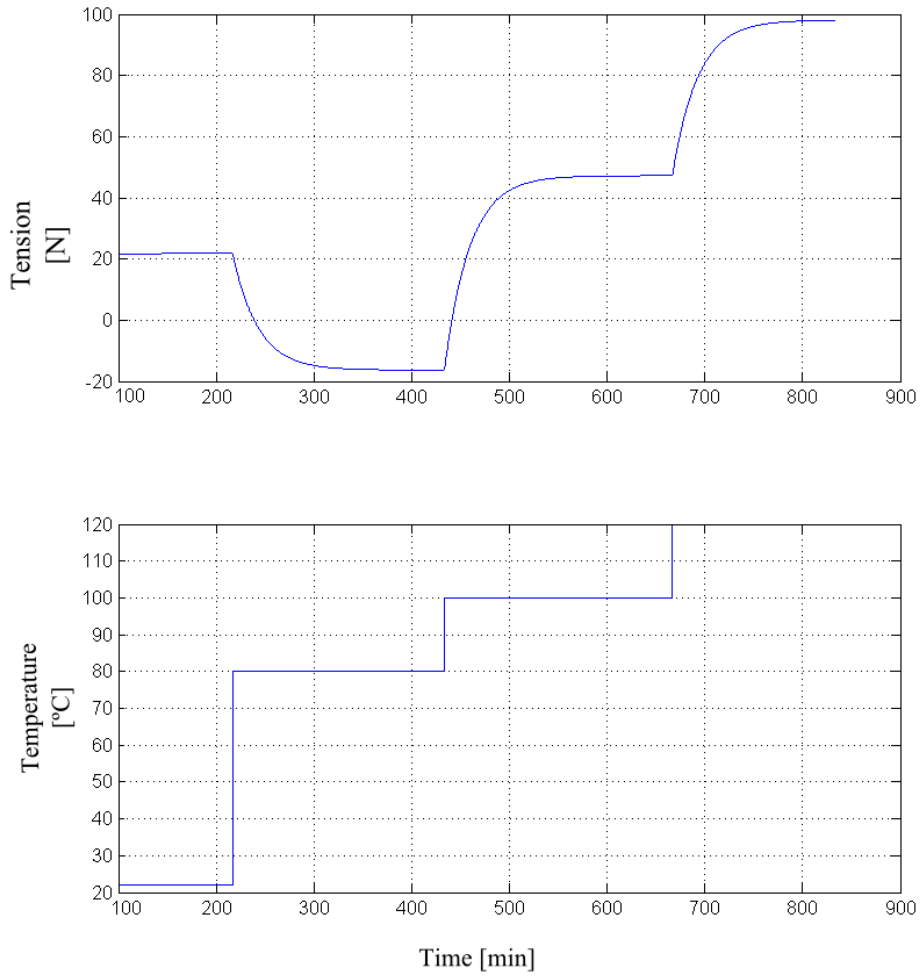

100

Figure 49. Simulation of tension change due to temperature change of 80 to 100 ºC and to 120 ºC. The simulation is given enough time to converge, which is expected to happen possibly faster in the real experiments .

The tension of the simulation seen in Figure 49 follows the trends that were proposed. Between 22 and 80 ºC the tension decreases because of expansion and the change of elastic modulus. In the next changes from 80 to 100 ºC and 100 to 120 ºC the tension rises because the web shrinks.

4.2 Experimental Results

The experiment with the previously mentioned parameters had the following results according to tension, time and temperature.

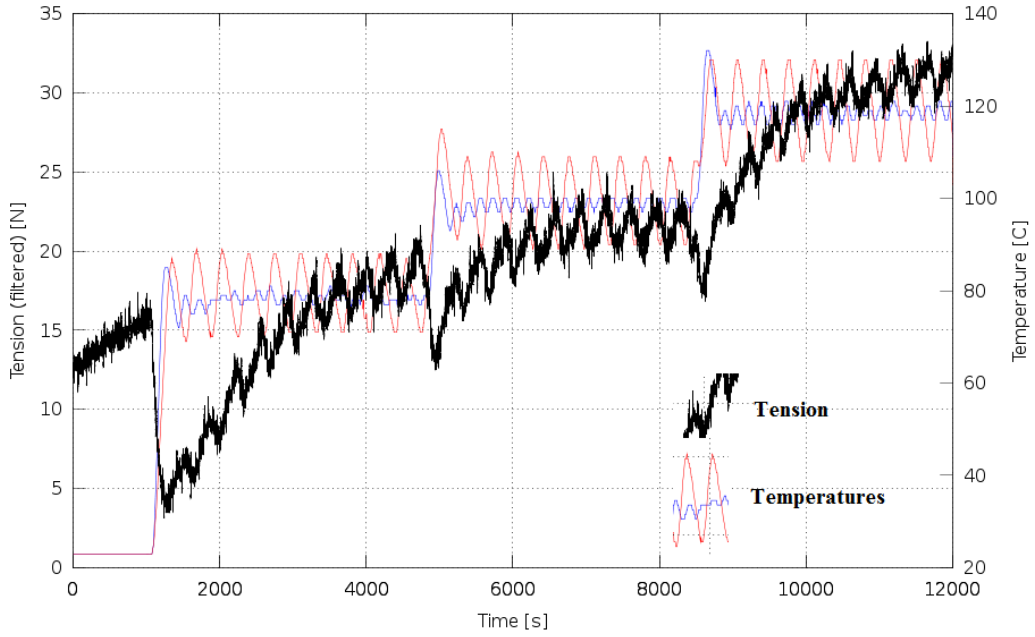

Figure 50. Tension and temperature according to time during the experiment. The blue temperature line, which is fluctuating less, is dryer 1, and the other one is dryer 2.

Here we can see the tension trend in the real system. The tension decreases during the first temperature change. After that, during the steady temperature region of 80 ºC, the tension keeps rising. When the tension reaches more of a steady state, the temperature is changed to 100 ºC, and the tension drops again, but not as dramatically as predicted by the hypothesis (Figure 50). The tension rises again during the steady temperature, and when the temperature rises to 120 ºC, the tension increases even more than at the last step.

4.3 Results of the Research

The tension model predicts the main direction of the change in tension, but not the scale. The previous simulations did not predict the slowly increasing tension during the steady states.

4.3.1 Analysing the Tension Model Compared to the Real System

The tension model was carefully crafted and checked. The thermal strain and tension drop of the web are at the same scale as in the previous studies by Lee et al. (2010), so mistakes in calculations are not expected. All the known properties of the web were taken into account, as functions of temperature and everything has been double checked. Let us study the possible differences between the simulation and the experiment:

(1) In the simulation, the time period is nearly 5 times longer than in the experiment. This can mean that, while in the simulation the system was given enough time to converge, in real life this might have not had enough time to happen. It is also possible that the simulation happens either slower or faster than in real life.

(2) We assume that the web will not have the exact temperature of the air in the dryer, and there should be a rising gradient of temperature in the oven compared to the distance travelled. There is a possibility that the dryer in fact does not raise the temperature of the web very high at all. One reason leading to this conclusion is that, according to measurements, the web coming out of the dryer 2 is only a little more than 50 ºC, while the air in the dryer is at 80 ºC. Then again, it is also possible that the web coming out of the dryer has already had time to cool down before coming out, especially with the extremely low speed of the web and the observation that there was not a lot of hot air coming out of the dryer.

Currently, there is no way to determine the real temperature of the web inside the dryer, as the laboratory does not have any sensors to ascertain this. The

assumption that the PET is 80 ºC is, of course, a rough estimate, and the change of the temperature in the PET must also be dependent on the change in the thermal conductivity of the material as a function of its temperature.

Also, considering that the incoming web is always at 22 ºC, but that it has the same time to heat up to 80 ºC as well as 120 ºC, this could mean that going to higher temperatures takes more time. Therefore, the higher the temperature in the dryer, the lower the average temperature of the web probably is compared to the air, because the web does not have enough time to heat up.

(3) We do not know the actual speeds of the experimental system's two pulling cylinders. The engines are DC-powered electric motors with speed controllers, but even the slightest speed change of less than millimetres per minute can drastically change the tension. It may be possible that the engine runs only slightly faster if it is given slack by the expanding web. Again, the speeds of the driving engines were of great interest to us, but we did not investigate this because of lack of equipment at the laboratory.

Their speeds are controlled by speed controllers, but the speeds are so extremely low, that it is possible that these controllers cannot reach the necessary control resolution. That resolution should be at least 10 µm / minute in order for it not to disturb the simulation.

4.3.2 **Simulation with the Estimated Temperature Values**

Let us consider a model where the real temperature data is input with 25 ºC removed from the higher temperatures and the speeds being constant.

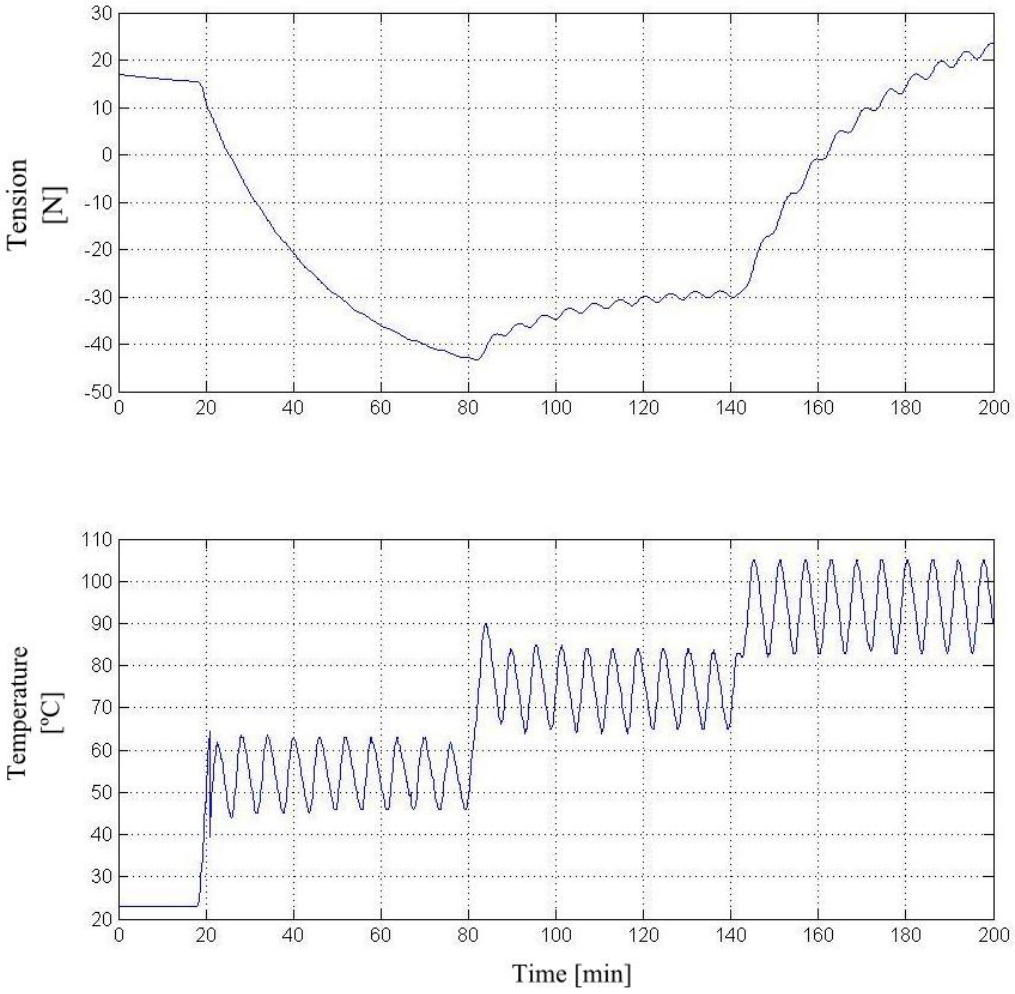

Figure 51. System where the real-time and temperature data with a lowered value of 25 ºC is used in the simulation.

The simulation responds by giving a more realistic final tension, and also showing increasing tensions at the steady states of 100 and 120 ºC (Figure 51). Nevertheless, the tension at the steady states of 24 and 80 degrees are going in the opposite direction to the real system (Figure 50). The real system must be more complicated, and there have to be more different variables affecting the span.

4.3.3 Final Simulation with Variation in the Cylinder Speeds

There is only one more variable we have not changed or measured, which is the speed of the cylinders. We do not know the actual speeds of the cylinders other than that they are supposed to be exactly 0.5 m / min. If the speed of the second cylinder is faster than that of the first one, it induces a positive tension change in the system. Let us iterate a simulation where the speed of the second cylinder moulds the simulation to be more like the real system.

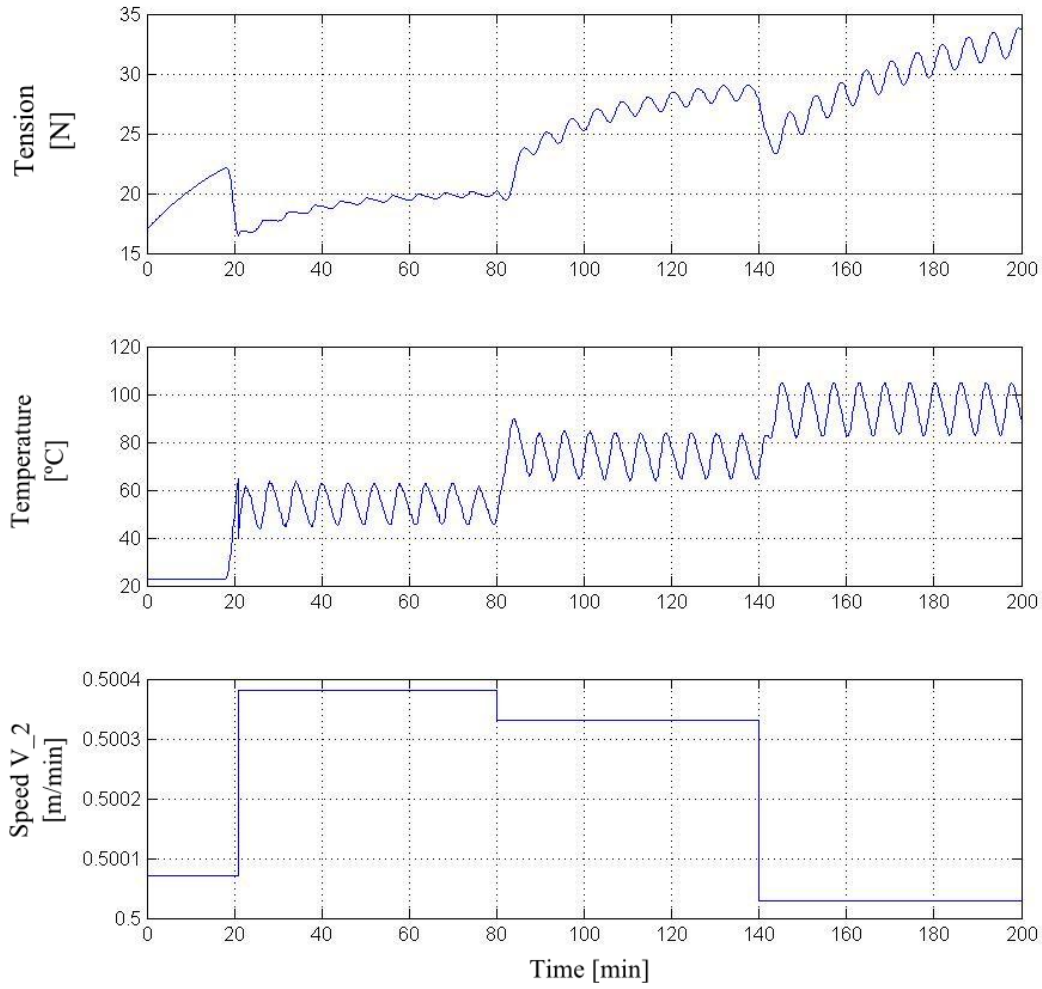

Figure 52. A simulation with a reduced real temperature profile and a moulded speed profile to make the system more like the experimental data.

Now the simulation represented in Figure 52 follows all the tendencies in the experimental system. Only the sudden tension drops were difficult to simulate, and this could be due to the fact that the system might have a slow reaction time to the web's properties. The speed change between 0 – 20 minutes is due to the fact that the real system also had a rising tension in the beginning. The next phase of 80 degrees might have a big speed change due to the fact that the web will experience expansion at this stage. As the temperature rises, the web will shrink and the speed of the second cylinder will slow down due to tightening.

The speeds of the driving cylinders have to be determined down to a precision of at least 10 µm / min to make sure they are not affecting the system. This way we will also know whether the speed controller needs more precision or adjustments. It should again be noted that these assumed speed changes are only on the scale of 0.1 – 0.4 mm / min or less than 0.1%. That is only 17 and 67 µm / s, which is an extremely small change.

Also it is crucial to determine the actual temperature of the PET inside the dryer at all positions, times and temperatures. It might be possible to determine the convection coefficients and thermal conductivities of PET to make a heat transfer model. A more sound approach would be to determine the temperature profile of the web inside the dryer from empirical evidence as a function of the distance travelled and temperature of the air.

5 CONCLUSIONS

According to observations and references the simulation can predict the tension in the web. The problem now is the lack of information about the system. Right now we are left with guesses of what happens inside the dryer but still a surprisingly accurate final output of the simulation.

The simulation represented in Figure 52 follows all the tendencies in the experimental system. Only the sudden tension drops were difficult to simulate, and this could be due to the fact that the system might have a slow reaction time to the web's properties. The speed change between 0 – 20 minutes is due to the fact that the real system also had a rising tension in the beginning. The next phase of 80 degrees might have a big speed change due to the fact that the web will experience expansion at this stage. As the temperature rises, the web will shrink and the speed of the second cylinder will slow down due to tightening.

The speeds of the driving cylinders have to be determined down to a precision of at least 10 µm / min to make sure they are not affecting the system. This way we will also know whether the speed controller needs more precision or adjustments. It should again be noted that these assumed speed changes are only on the scale of 0.1 – 0.4 mm / min or less than 0.1%. That is only 17 and 67 µm / s, which is an extremely small change.

Also it is crucial to determine the actual temperature of the PET inside the dryer at all positions, times and temperatures. It might be possible to determine the convection coefficients and thermal conductivities of PET to make a heat transfer model. A more sound approach would be to determine the temperature profile of the web inside the dryer from empirical evidence as a function of the distance travelled and temperature of the air.

BIBLIOGRAPHY

GSM Arena. 2012. Nokia Demonstrates Flexible OLED Display [Web blog] [Retrieved July 11th, 2012]. Available at http://www.gsmarena.com/nokia_demonstrates_flexible_oled_display_at_nokia_world-news-3318.php

Bock, K., Klink, G., Strohhofer, C., Hemmetzberger, D. & Feil, M. 2007. Large Area Cost-Efficient Electronics Systems Integration. Electronic Components and Technology Conference (ECTC '07), Munich, May 29 - June 1. IEEE. pp. 1540-1543.

Cheng, I.-C. & Wagner, S. 2009. Overview of Flexible Electronics Technology. In W. S. Wong (Ed.), Flexible Electronics, Vol. 11, p. 28. Springer US.

Choi, K., Tran, T., Ganeshthangaraj, P., Lee, K., Nguyen, M., Jo, J.D. & Kim, D. S. (2010). Web register control algorithm for roll-to-roll system based printed electronics. Conference on Automation Science and Engineering (CASE), Aug 21-29, IEEE. Jeju, South Korea: IEEE.

Hrehorova, E., Rebros, M., Pekarovicova, A., Bazuin, B. & Ranganathan, A. 2011. Gravure Printing of Conductive Inks on Glass. Journal of Display Technology, Vol. 7, No. 6.

IDTechEx. 2012. Glossary: Offset lithography. [Web page] [Retrieved July 26th, 2012] Available at http://www.printedelectronicsworld.com/glossary/offset-lithography-160.asp?sessionid=1

Incropera, F. P., Dewitt, D. P., Bergman, T. L. & Lavine, A. S. 2006. Fundamentals of Heat and Mass Transfer. USA: John Wiley & Sons.

Kang, H. 2000. Two-dimensional modeling and control for multi-layer roll-to-roll printing systems. Seoul, Korea: Konkuk University.

Kang, H.-K., Lee, C.-W., Lee, J.-M. & Shin, K.-H. 2009. Cross direction register modeling and control in a multi-layer gravure printing. Seoul, Korea: Springer. Journal of Mechanical Science and Technology, Vol. 24, No. 1.

Keng, L. B., Lai, W. L., Lu, C. & Salam, B. 2011. Processing and characterization of flexographic printed conductive grid. Electronics Packaging Technology Conference (EPTC) IEEE 13th, December 7-9,. Singapore. IEEE. pp. 517-520.

Kim, C.-H., You, H.-I., Lee, S.-H. & Jo, J. 2011. Design of Multi-Purposed Roll-to-Roll Printing System for Printed Electronics. 8th International Conference on Ubiquitous Robots and Ambient Intelligence (URAI), November 23-26, Songdo, Incheon, Korea. IEEE. pp. 690-691.

Krebs, F. C. 2009. Fabrication and processing of polymer solar cells: A review of printing and coating techniques. Denmark, Elsevier. Solar EnergyMaterials & Solar Cells, Vol. 93.

Krumm, J. & Clemens, W. 2011. Printed Electronics—First Circuits, Products, and Roadmap. Analog Circuit Design 2011. Netherlands. Springer Science+Business Media B.V.

Kutz, M. 2011. Applied Plastics Engineering Handbook, processing and materials (1st ed.). Kidlington, UK: Elsevier Inc.

Lee, C., Kang, H. & Shin, K. 2009. A study on tension behavior considering thermal effects in roll-to-roll E-printing. Springerlink.com. Journal of Mechanical Science and Technology Vol. 24 No. 5.

Lin, K. H., Xu, Z. H. & Tian, L. S. 2011. A Study on Microstructure and Dielectric Performances of Alumina/Copper Composites by Plasma Spray Coating. Springer US. Journal of Materials Engineering and Performance. Vol. 20. No. 2.

Luo, W., Hu, W. & Xiao, S. 2008. Size Effect on the Thermodynamic Properties of Silver Nanoparticles. Web journal. American Chemical Society. The Journal of Physical Chemistry C. Vol. 112.

Löher, T., Vieroth, R., Seckel, M., Ostmann, A. & Reichl, H. 2008. Stretchable electronic Systems for wearable and textile Applications. VLSI Packaging Workshop of Japan (VPWJ) IEEE 9th, December 1-2. IEEE. pp. 9-12.

Maekawa, K., Yamasaki, K., Niizeki, T., Mita, M., Matsuba, Y., Terada, N. Saito, H. 2012. Drop-on-Demand Laser Sintering With Silver Nanoparticles for Electronics Packaging. Components, Packaging and Manufacturing Technology, IEEE Transactions on. Vol. 2. No. 5. pp. 868-677.

McGoldrick, K. 2006. Mobile Friendly Rollable Displays. Solid-State Circuits Conference,. ESSCIR. Proceedings of the 32nd European. Eindhoven, The Netherlands: IEEE. pp. 1-2.

Mens, R., Adriaensens, P., Lutsen, L., Swinnen, A., Bertho, S., Ruttens, B., D'Haen, J., Manca, J., Cleij, T., Vanderzande, D. & Gelan, J. 2007. NMR Study of the Nanomorphology in Thin Films of Polymer Blends Used in Organic PV Devices: MDMO-PPV/PCBM. Journal of Polymer Science Part A: Polymer Chemistry, Vol. 46.

Montgomery, D. C. 2009. Design and Analysis of Experiments. USA: John Wiley & Sons.

Moore, G. E. 1965. Cramming more components onto integrated circuits. Electronics, Vol. 38, No. 4.

NANO Observatory. 2010. ICT Sector Focus Report, Printed Electronics. [ICT Sector Focus Report] [Retrieved July 26th, 2012]. Available at http://www.observatorynano.eu/project/filesystem/files/ObservatoryNanoFocusReport_PrintedElectronics.pdf

Numakura, D. 2008. Advanced Screen Printing "Practical Approaches for Printable & Flexible Electronics". 3rd International Microsystems, Packaging, Assembly & Circuits Technology Conference (IMPACT), October 22-24, Taipei. IEEE. pp. 205-208.

Optomec. 2006a. Aerosol jet is not inkjet. [Web page]. [Retrieved July 25th, 2012]. Available at http://www.optomec.com/Additive-Manufacturing-Technology/Inkjet

Optomec. 2006b. Aerosol Jet Technology. [Web page]. [Retrieved July 25th, 2012]. Available at http://www.optomec.com/Additive-Manufacturing-Technology/Printed-Electronics

Peckham, M. 2012. The Collapse of Moore's Law: Physicist Says It's Already Happening. [Web page]. [Retrieved July 23rd 2012]. Available at http://techland.time.com/2012/05/01/the-collapse-of-moores-law-physicist-says-its-already-happening/

Pinto, M. R., W., Brinkman, W. F. & Troutman, W. W. (n.d.). The Transistor's Discovery and What's Ahead. [Web Magazine]. [Retrieved July 9th, 2012]. Available at http://www.imec.be/essderc/papers-97/322.pdf

Pudas, M., Hagberg, J. & Leppavuori, S. 2002. The absorption ink transfer mechanism of gravure offset printing for electronic circuitry. IEEE Transactions on Electronics Packaging Manufacturing. Oulu. IEE Expolore. Vol. 25, No. 4.

Ryu, K., Badmaev, A. & Zhou, C. 2008. Flexible and Wearable Devices based on Transferred Aligned Carbon Nanotube Arrays, Device Research Conference, June 23-25, Santa Barbara, CA, USA. IEEE. pp. 21-22.

Sabu, T. & Visakh, P. 2011. Vol. 3: Polyethers and Polyesters. In Handbook of Engineering and Specialty Thermoplastics. Hoboken NJ, USA. Wiley.

Sadd, M. H. 2009. Appendix D: Review of Mechanics of Materials. In Elasticity - Theory, Applications, and Numerics (2nd Edition). Elsevier Science & Technology.

Shin, K.-H. 1991. Distributed Control of Tension in Multi-Span Web Transport Systems. Doctor's dissertation. Oklahoma: Oklahoma State University, Department of mechanical Engineering.

Singh, T. 2010. LG's flexi-electronic newspaper. [Web Newspaper Article]. [Retrieved July 12th, 2012]. Available at http://www.ngonlinenews.com/news/e-newspapers/

Southee, D., Hay, G., Evans, P. & Harrison, D. 2007. Printed Electronics and Offset Lithography, Innovative Electronics Manufacturing Seminar, Electronics Yorkshire June 26. [Seminar Presentation]. [Retrieved July 26th, 2012]. Available at http://www.lboro.ac.uk/research/iemrc/documents/EventsDocuments/Printed_Electronics.pdf

Spielberg, S. (Director). 2002. Minority Report [Motion Picture].

Suganuma, K., Wakuda, D., Hatamura, M. & Kim, K.-S. 2007. Ink-jet Printing of Nano Materials and Processes for Electronics Applications. International Symposium on High Density packaging and Microsystem Integration (HDP '07). June 26-28. Shanghai. IEEE.

Technology-Update.us. 2010. SAMSUNG Un-breakable and Flexible AMOLED Display. [Youtube video]. [Retrieved July 20th, 2012]. Available at http://www.youtube.com/watch?v=pzq0rKK5Kb0

Tobjörk, D. & Österbacka, R. 2011. Paper Electronics. Graduate school of materials research, Center of Functional materials research. Turku, Finland: Advanced Materials. Vol. 23. No. 17.

The Engineering Toolbox. 2012. Radiation Heat Transfer. [Web page]. [Retrieved August 21st, 2012] Available at http://www.engineeringtoolbox.com/radiation-heat-transfer-d_431.html

Tunlasakun, K. & Makasorn, P. 2008. Solar powered EL traffic police vest. Control, Automation and Systems, 2008. International Conference on Control, Automation and Systems (ICCAS), October 14-17, Seoul Korea. IEEE. pp. 1337-1340.

Yang, Y., Chang, S.-C., Bharathan, J. & Liu, J. 2000. Organic/polymeric electroluminescent devices processed by hybrid ink-jet printing. Department of Materials Science and Engineering, University of California. Kluwer Academic Publishers. Journal of Materials Science: Materials in Electronics. Vol. 11. pp. 89-96.

Yin, Z., Huang, Y., Bu, N., Wang, X. & Xiong, Y. 2010. Inkjet printing for flexible electronics: Materials, processes and equipments. State Key Laboratory of Digital Manufacturing Equipment and Technology, Huazhong University of Science and Technology. Science China Press and Springer-Verlag Berlin Heidelberg 2010. Chinese Science Bulletin, Vol. 55 No. 30.

Zhang, R. & Wong, C. 2009. Advanced interconnect materials for ink-jet printing by low temperature sintering. Electronic Components and Technology Conference (ECTC). May 26-29. Atlanta, USA. IEEE. pp. 150-154.

Appendix 1. Perturbation of the Unlinear Tension Equation

Here is the unlinear equation from Chapter 3.8 which we will perturbate:

$$\frac{d}{dt}[t_2(t)] = -\frac{v_2(t)}{L}t_2(t) + \frac{v_1(t)}{L} \times t_1(t) + \frac{A \times \sum_{i=1}^{3}\left[E_i(t) \times \frac{L_i}{L}\right]}{L}[v_2(t) - (v_1(t)] - \frac{A \times \sum_{i=1}^{3}\left[E_i(t) \times \frac{L_i}{L} \times \in_i^t\right]}{L} v_2(t) \quad (52)$$

Now let us break this equation down by making some assumptions:

(1) The upstream stress t_1 is a constant.

(2) Thermal strain in the span parts 1 and 3 are very close to zero (This was proven by temperature measurements).

In order to linearize let us make the following assumption:

$$v_1(t) = v_1(t) + v_{10} \quad (53)$$

$$v_2(t) = v_2(t) + v_{20} \quad (54)$$

$$t_2(t) = t_2(t) + t_{20} \quad (55)$$

$$E(t) = E(t) + E_0 \quad (56)$$

$$\in_2^t (t) = \in_2^t (t) + \in_{20}^t \quad (57)$$

We can simplify the equation with the above functions as well as apply the Hooke's law:

(Continues)

(Appendix 1 continues)

$$\frac{L}{A}\frac{d}{dt}[T_2(t)] = v_1(t) \times T_1 + t_2(t)v_2(t) + T_2(t)v_{20} + t_{20}v_2(t) + t_{20}v_{20} + E(t)v_2(t) - E(t)v_{20} - E_0v_2(t) + E_0v_2(t) + E_0v_{20} + E(t)v_1(t) \mp E(t)v_{10} + E_0v_1(t) + E_0v_1(t) + E_0v_{10} - E_2(t) \in_2^t (t)v_2(t) + E_2(t) \in_{20}^t v_2(t) + E_{20} \in_2^t (t)v_2(t) - E_{20} \in_{20}^t v_2(t) + E_2(t) \in_2^t (t)v_{20} - E_2(t) \in_{20}^t v_{20} - E_0 \in_2^t (t)v_{20} + E_0 \in_{20}^t v_{20} \quad (58)$$

Now to satisfy the initial steady state condition:

$$0 = t_{20}v_{20} + E_0v_{20} + E_0v_{10} + E_0 \in_{20}^t v_{20} \quad (59)$$

We can remove all these elements from the equation. Also we can assume that $\in_{20}^t$ is zero, as in the simulation the temperature is the same as room temperature in the beginning.

Another way to simplify the equation is to remove all elements with second or third degree variables. When multiplying two or three small changes together we can assume that the result is very close to zero.

Then we get the following equation:

$$\frac{d}{dt}[T_2(t)] = -\frac{v_{20}}{L}T_2(t) + \frac{v_{10}}{L}T_1(t) + \frac{A \times \sum_{i=1}^{3} E_i(t)\frac{L_i}{L}}{L}[V_{20} - V_{10}] + \frac{A \times \sum_{i=1}^{3} \bar{E}_{i0}\frac{L_i}{L}}{L}[V_{20}(t) - (V_{10}(t)] - \frac{A \times E_2 \times \in_2^t (t) \times \frac{L_2}{L}}{L}V_{20} \quad (60)$$

From which we can once more remove the second element $\frac{A \times \sum_{i=1}^{3} E_i(t)\frac{L_i}{L}}{L}[V_{20} - V_{10}]$ because we have decided that the speeds of the cylinders in the beginning are the same. The final perturbated equation is as follows.

(Continues)

(Appendix 1 Continues)

$$\frac{d}{dt}[T_2(t)] = -\frac{v_{20}}{L}T_2(t) + \frac{v_{10}}{L}T_1(t) + \frac{A\times\sum_{i=1}^{3}\bar{E}_{i0}\frac{L_i}{L}}{L}[V_{20}(t) - (V_{10}(t)] - \frac{A\times E_2\times\in_2^t(t)\times\frac{L_2}{L}}{L}V_{20} \quad (61)$$